Multiscale numerical method for nonlinear Maxwell equations.

T. Colin[‡] and B. Nkonga [‡]

[‡] MAB: Mathématiques Appliquées de Bordeaux, UMR CNRS 5466,
Univ. Bordeaux 1, 33405 Talence cedex,
colin@math.u-bordeaux1.fr nkonga@math.u-bordeaux1.fr

Abstract

The aim of this work is to propose an efficient numerical approximation of high frequency pulses propagating in nonlinear dispersive optical media. We consider the nonlinear Maxwell's equations with instantaneous nonlinearity. We first derive a physically and asymptotically equivalent model that is semi-linear. Then, for a large class of semi-linear systems, we describe the solution in terms of profiles. These profiles are solution of a singular equation involving one more variable describing the phase of the solution. We introduce a discretization of this equation using finite differences in space and time and an appropriate Fourier basis (with few elements) for the phase. The main point is that accurate solution of the nonlinear Maxwell equation can be computed with a mesh size of order of the wave length. This approximation is asymptotic-preserving in the sense that a multi-scale expansion can be performed on the discrete solution and the result of this expansion is a discretization of the continuous limit. In order to improve the computational delay, computations are performed in a window moving at the group velocity of the pulse. The second harmonic generation is used as an example to illustrate the proposed methodology. However, the numerical method proposed for this benchmark study can be applied to many other cases of nonlinear optics with high frequency pulses.

keywords: Interactions laser-matter, localized pulses, Maxwell's equations, nonlinear optics, WKB.

1 Introduction

The recent development of the laser pulsed with intense energy increases the need of modelization and simulation [6, 18, 14, 20, 24, 26]. At high intensities, new regimes

of laser-matter interaction are explored in a variety of fields of application: selective ionization of multilevel atomic systems [9], spontaneous and simulated Raman and Brillouin scattering [23], plasma, CFI, ... Numerical simulation are much cheaper to use than real experiments. However a wide set of regimes have to be considered: the wavelength associated to a pulse is usually near the micrometer (10^{-6}m) while the length of the pulse can be of order of 100 micrometers for ultrashort pulses (10^{-4}m) or of the order of the meter. We are concerned with propagation on distances of order of the millimeter (for crystals) or of hundred of meters (for propagation in gas). From the temporal point of view, the pulsation of a pulse is $10^{15}s^{-1}$, its duration can be of the order of the picoseconds ($10^{-12}s$) or of 10 nanoseconds ($10^{-8}s$). The duration of propagation can be $10^{-11}s$ for crystals or $10^{-6}s$ for gas. The width of the beam can be of order of a fraction of millimeter to a few centimeters. Therefore, one has to handle 3D processes involving several orders of magnitude. No general method is available for all this class of problems. A first class of methods is to use the so-called par-axial approximation or envelope approximation. This approximation relies on the fact that the electric field can be thought under the form

$$e^{i(kz-\omega t)}\mathcal{E}(t,x,z) \text{ with } \partial_t\mathcal{E} << \omega\mathcal{E}, \quad \partial_x\mathcal{E} << k\mathcal{E}, \quad \partial_z\mathcal{E} << k\mathcal{E}.$$

Using these inequalities, one obtains approximate equations satisfied by $\mathcal{E}$. These equations can be nonlinear transport equations at the group velocity (for frequency doubling in the phase-matching case in a crystal) or nonlinear Schrödinger equations (in a Kerr medium) or Schrödinger-Bloch equations (in a gas) ... We refer to general textbook of physics ([6], [20] for instance) for a precise physical description.

When one wants to address cases where the validity of the par-axial approximation is not so clear, another strategy can be used. Physically, it can occur when the pulse goes through a diffraction web or when the pulse is "chirped" in order to have a large spectral width. The first possibility is to use standard FDTD approach on nonlinear Maxwell type systems. However, the cost in terms of time of computation is very high and one could have some problem in order to ensure numerical phase-matching. We want to propose here an alternative intermediate method that is more precise than the usual Schrödinger-like equation but less expansive to compute numerically than the full Maxwell's equations. We present this method in this paper and we apply it to the second harmonic generation of a femtosecond high intensity laser pulse centered around a given carrier frequency ω in a noncentrosymmetric KDP (Potassium Di hydrogen Phosphate) crystal with a large second-order susceptibility.

The method that we present in this paper relies on ideas of Joly, Métivier and Rauch of the last decade. The electromagnetic field corresponding to a laser pulse can be written under the form

$$u(t,x) = \left(e^{i\frac{k\cdot X-\omega t}{\varepsilon}}A(t,X) + c.c.\right), \tag{1.1}$$

where *c.c.* denotes the conjugate complex, k is the wave vector, ω the frequency, $X \in \mathbb{R}^n$ is the space variable and t is the time. The vector A belongs to $\mathbb{R}^p$ for some integer p and contains the electric field, the magnetic field and possibly auxilliary fields useful to describe the interaction of the light with the medium. See below for example. In a dispersive medium, the relationship between ω and k is non linear and is called the dispersion relation. Of course, in nonlinear media, other harmonics are created and the solution can be more complicated. The electromagnetic field is a solution to a semi linear Maxwell system describing the evolution of laser pulses in nonlinear medium which enters the following family of systems:

$$\left(\partial_t + A(\partial_X) + \frac{L_0}{\varepsilon}\right) u = f(u), \tag{1.2}$$

where $u : [0,T] \times \mathbb{R}^n \to \mathbb{R}^p$

$$A(\partial_X) = \sum_{j=1}^{n} A_j \partial_{x_j}, \quad f : \mathbb{R}^p \to \mathbb{R}^p.$$

Matrices A_j are symmetric, L_0 is skew-symmetric, f is a smooth mapping and $\varepsilon > 0$ is a small parameter which is related to the order of magnitude of the wavelength. System (1.2) is endowed with an initial data $u(0,x) = e^{i\frac{k\cdot X}{\varepsilon}} A(0,X) + c.c.$
One has therefore to compute solutions to (1.2). Since the solution has an oscillatory behavior, the number of discretization points in x has to be large with respect to $\frac{1}{\varepsilon}$ and the number of time steps has also to be large with respect to $\frac{1}{\varepsilon}$. Direct computations of solutions to (1.2) are therefore very hard and lead to large computational times. In order to overcome this difficulty, one can use the par-axial approximation which consists essentially in using (1.1) and writing

$$A(t,X) \approx A_0(\varepsilon t, X - \omega'(k)t),$$

and proving that $A_0(\tau, y)$ satisfies a nonlinear Schrödinger equation (see [11]). When this approximation is suspected not to be valid, one has really to use (1.2). The method we propose here uses the structure of a laser pulse. We consider that the solution $u^\varepsilon(t,X)$ of (1.2) is given by a profile $\mathcal{U}^\varepsilon(t,X,\theta)$ as follows:

$$u^\varepsilon(t,X) = \mathcal{U}^\varepsilon(t,X,\frac{k\cdot X - \omega t}{\varepsilon})$$

where $\theta \mapsto \mathcal{U}^\varepsilon(t,X,\theta)$ is periodic. We therefore consider that $\mathcal{U}^\varepsilon$ is given by all its harmonics in the rapid variable. One thus expects that the variations of

$$(t,X,\theta) \mapsto \mathcal{U}^\varepsilon(t,X,\theta)$$

are moderate so that the number of discretization points has not to be large with respect to $\frac{1}{\varepsilon}$. Of course one has to add a space dimension at the initial problem (the phase variable). But usually, only a few harmonics are necessary in order to characterize the solution (less than 5 in any practical case). The discretization in the θ variable will therefore be cheap in terms of computational cost. The equation satisfied by $\mathcal{U}^\varepsilon$ is the following singular equation:

$$\left(\partial_t - \frac{\omega}{\varepsilon}\partial_\theta + \frac{1}{\varepsilon}A(\varepsilon\partial_X + k\partial_\theta) + L_0)\right)\mathcal{U}^\varepsilon = f(\mathcal{U}^\varepsilon). \tag{1.3}$$

Solving (1.3), we compute an exact solution of the complete nonlinear system and not a function given by an envelope approximation. Moreover, we show that the discretized version of (1.3) also admits an asymptotic expansion and we prove that this expansion is a discretized version of the envelope equation.

This paper is organized as follows:
In Section 2, we introduce the Maxwell-Lorentz system describing the propagation of a laser beam in a nonlinear medium with quadratic nonlinearity: even if it seems to be rude, we give all the values of the coefficients in a physical realistic situation. We describe the phase-matching condition. This model is quasilinear. We derive a physically equivalent model which is semi-linear and is of the form (1.2).
In Section 3, we recall some basic facts on WKB expansion. We next introduce our semi-discretization in time on the full semi-linear Maxwell's system using the singular equation (1.3). We prove an error estimate and we show that this numerical method can be seen as a numerical multi-scale method that is asymptotic-preserving in the sense that the discretization of the limit is the limit of the discretization.
In Section 4, we present the total discretization, the moving window technique and some numerical results.

2 Nonlinear Maxwell-Lorentz equations for a noncentrosymmetric crystal

The aim of this section is to write a system of nonlinear equations of Maxwell-Lorentz type describing the evolution of a laser beam in a nonlinear, noncentrosymmetric crystal. Such a crystal is characterized by different indexes corresponding to the directions of the axis of the crystal. We have therefore to include in the model the position of the crystal with respect to the beam. This will be done by giving the rotation matrix that allows to transform the laboratory coordinates into the crystallographic ones.

2.1 Setting of the equations

Let θ and φ be the two angles describing the geometrical position of the crystal with respect to the propagation direction of the laser. We consider the physical coordinates denoted by $X = (x, y, z)$ and the crystallographic coordinates $\Xi = (\xi, \eta, \zeta)$ defined by $\Xi = \mathbb{P}X$, where $\mathbb{P}$ is a rotation matrix defined by the angles θ and φ:

$$\mathbb{P} = \begin{pmatrix} \cos(\varphi)\cos(\theta) & -\sin(\theta) & \sin(\varphi)\cos(\theta) \\ \cos(\varphi)\sin(\theta) & \cos(\theta) & \sin(\varphi)\sin(\theta) \\ -\sin(\varphi) & 0 & \cos(\varphi) \end{pmatrix}.$$

The electric field $\mathcal{E}(t, X)$, magnetic field $\mathcal{H}(t, X)$ and electric flux density $\mathcal{D}(t, X)$ are functions of the coordinate X but their components are formulated in the crystallographic coordinates. For example, if $E(t, X)$ is the electric field in the physical coordinates we have:

$$\mathcal{E}(t, X) = \mathbb{P}E(t, X) = (\ \mathcal{E}_\xi(t, X),\ \mathcal{E}_\eta(t, X),\ \mathcal{E}_\zeta(t, X))^T.$$

This transformation is introduced in order to simplify the formulation of the nonlinear polarization.

Maxwell's equations, describing the wave propagation in a nonlinear medium with no free charge are then expressed by:

$$\begin{cases} \partial_t \mathcal{H} & + & \dfrac{1}{\mu_0}\left(\mathcal{M}_x\partial_x\mathcal{E} + \mathcal{M}_y\partial_y\mathcal{E} + \mathcal{M}_z\partial_z\mathcal{E}\right) = 0, \\ \partial_t \mathcal{D} & - & \dfrac{1}{\epsilon_0}\left(\mathcal{M}_x\partial_x\mathcal{H} + \mathcal{M}_y\partial_y\mathcal{H} + \mathcal{M}_z\partial_z\mathcal{H}\right) = 0, \end{cases} \tag{2.4}$$

where μ_0 is the free space permeability and ε_0 the free space permeability. The constitutive relation is:

$$\mathcal{D} = \mathcal{P}^{(1)}(\mathcal{E}) + \mathcal{P}^{(2)}(\mathcal{E}),$$

where $\mathcal{P}^{(1)}$ and $\mathcal{P}^{(2)}$ are the linear and the quadratic polarizations in the crystallographic coordinates. We now explain how to compute these terms. As usual, (see [6] for example), $\mathcal{P}^{(1)}$ and $\mathcal{P}^{(2)}$ are given by $\mathcal{P}^{(1)} = \chi^{(1)}(\mathcal{E})$ and $\mathcal{P}^{(2)} = \chi^{(2)}(\mathcal{E}, \mathcal{E})$ where $\chi^{(1)}$ and $\chi^{(2)}$ are respectively second and third order tensors eventually depending of the frequency, see below for a precise meaning of this dependence.

• For $\mathcal{P}^{(2)}$, we take a third order tensor $\chi^{(2)}$ with constant coefficients. For the crystal of the $\overline{4}$2m point group, considered in these investigations, the quadratic polarization thus obtained is :

$$\mathcal{P}^{(2)}(\mathcal{E}) = \begin{pmatrix} d_{24}\ \mathcal{E}_\eta\ \mathcal{E}_\zeta \\ d_{24}\ \mathcal{E}_\xi\ \mathcal{E}_\zeta \\ d_{36}\ \mathcal{E}_\xi\ \mathcal{E}_\eta \end{pmatrix}, \tag{2.5}$$

where $d_{24} = 2\chi^{(2)}_{\xi\eta\zeta} = 2\chi^{(2)}_{\xi\zeta\eta} = 2\chi^{(2)}_{\eta\xi\zeta} = 2\chi^{(2)}_{\eta\zeta\xi}$, $d_{36} = 2\chi^{(2)}_{\zeta\xi\eta} = 2\mathcal{X}^{(2)}_{\zeta\eta\xi}$. The numbers d_{24} and d_{36} are taken to be equal here and are given by

$$d_{24} = d_{36} = 4(4.35 \times 10^{-13})m/V.$$

• For the linear part $\mathcal{P}^{(1)}$, the situation is more complicated. The linear dispersion is characterized by the two Lorentz resonances (indexed by a and b). The linear polarization is defined via a Fourier transform in time: $\mathcal{F}(\mathcal{P}^{(1)})(\omega) = \chi^{(1)}(\omega)\mathcal{F}(\mathcal{E}(\omega))$, where $\mathcal{F}$ denotes the Fourier transform with respect to the time variables. The function $\chi^{(1)}(\omega)$ is given by

$$\chi^{(1)}(\omega) = \chi^{(1)}_{\infty} + \alpha_a\chi^{(1)}_a(\omega) + \alpha_b\chi^{(1)}_b(\omega).$$

The tensors $\chi^{(1)}_{\infty}$, α_a and α_b are second order diagonal tensors with constant coefficients satisfying the relation $\alpha_a + \alpha_b = Id$. The tensors $\chi^{(1)}_a(\omega)$ and $\chi^{(1)}_b(\omega)$ are given by

$$\chi^{(1)}_a(\omega) = \left(\frac{\chi^{(1)}_s - \chi^{(1)}_{\infty}}{1 - \frac{\omega^2}{\omega_a^2}}\right), \qquad \chi^{(1)}_b(\omega) = \left(\frac{\chi^{(1)}_s - \chi^{(1)}_{\infty}}{1 - \frac{\omega^2}{\omega_b^2}}\right),$$

where ω_a and ω_b are the diagonal tensors of angular velocities associated with the Lorentz resonance frequencies. Moreover $\chi^{(1)}_s$ is a diagonal tensor with constant coefficients. Using an inverse Fourier transform, the linear polarization writes as:

$$\mathcal{P}^{(1)} = \chi^{(1)}_{\infty}\mathcal{E} + \alpha_a\mathcal{F} + \alpha_b\mathcal{G}, \tag{2.6}$$

where the residual linear dispersions $\mathcal{F}$ and $\mathcal{G}$ satisfy the following second order differential equations:

$$\partial_t^2\mathcal{F} + \omega_a^2 \cdot \mathcal{F} = \alpha_a\omega_a^2 \cdot \mathcal{T}\mathcal{E}, \quad \text{and} \quad \partial_t^2\mathcal{G} + \omega_b^2 \cdot \mathcal{G} = \alpha_b\omega_b^2 \cdot \mathcal{T}\mathcal{E}, \tag{2.7}$$

with $\mathcal{T}\mathcal{E} = (\chi^{(1)}_s - \chi^{(1)}_{\infty}) \cdot \mathcal{E}$.

The Maxwell-Lorentz system is now completely defined. For one dimension applications, the model can be written in the form:

$$\left\{\begin{array}{lllllll} \partial_t\mathcal{H} & + & \mathcal{M}\partial_z\mathcal{E} & & & = & 0, \\ \chi^{(1)}_{\infty}\partial_t\mathcal{E} & - & c^2\mathcal{M}\partial_z\mathcal{H} & + & \omega_a\mathcal{U} + \omega_b\mathcal{V} & = & -\partial_t\mathcal{P}^{(2)}(\mathcal{E}), \\ \partial_t\mathcal{F} & & & - & \omega_a\mathcal{U} & = & 0, \\ \partial_t\mathcal{G} & & & - & \omega_b\mathcal{V} & = & 0, \\ \partial_t\mathcal{U} & + & \omega_a\mathcal{F} & - & \alpha_a\omega_a\mathcal{T}\mathcal{E} & = & 0, \\ \partial_t\mathcal{V} & + & \omega_b\mathcal{G} & - & \alpha_b\omega_b\mathcal{T}\mathcal{E} & = & 0. \end{array}\right. \tag{2.8}$$

The matrix $\mathcal{M}$ is given by

$$\mathcal{M} = \begin{pmatrix} 0 & -\cos(\varphi) & \sin(\varphi)\sin(\theta) \\ \cos(\varphi) & 0 & -\sin(\varphi)\cos(\theta) \\ -\sin(\varphi)\sin(\theta) & \sin(\varphi)\cos(\theta) & 0 \end{pmatrix}.$$

For the KDP crystal that we consider in this paper, the numerical values are

$$\chi_\infty^{(1)} = \begin{pmatrix} 1.4797154 & 0 & 0 \\ 0 & 1.4797154 & 0 \\ 0 & 0 & 1.4293487 \end{pmatrix},$$

$$\chi_s^{(1)} = \begin{pmatrix} 15.264496 & 0 & 0 \\ 0 & 15.264496 & 0 \\ 0 & 0 & 5.3606604 \end{pmatrix},$$

$$\alpha_a = \begin{pmatrix} 0.0565523 & 0 & 0 \\ 0 & 0.0565523 & 0 \\ 0 & 0 & 0.1789019 \end{pmatrix},$$

$$\alpha_b = \begin{pmatrix} 0.9434477 & 0 & 0 \\ 0 & 0.9434477 & 0 \\ 0 & 0 & 0.8210981 \end{pmatrix},$$

and finally the resonance's frequencies are

$$\omega_a = \begin{pmatrix} 1.6568042 \times 10^{16} & 0 & 0 \\ 0 & 1.6568042 \times 10^{16} & 0 \\ 0 & 0 & 1.7008821 \times 10^{16} \end{pmatrix},$$

$$\omega_b = \begin{pmatrix} 0.9423375 \times 10^{14} & 0 & 0 \\ 0 & 0.9423375 \times 10^{14} & 0 \\ 0 & 0 & 0.9423375 \times 10^{14} \end{pmatrix}.$$

2.2 Phase matching

In this section, we restrict our investigations to the linear regime. We consider plane wave of the form

$$\mathcal{E}(z,t) = \mathcal{E}_0 e^{i(kz-\omega t)}.$$

The vector amplitude $\mathcal{E}_0$ of the electrical field satisfies the following linear system:

$$\left(\omega^2 \chi^{(1)}(\omega) + k^2 \mathcal{M}^2\right) \mathcal{E}_0 = 0. \tag{2.9}$$

Since it is assumed that the wave is propagating in the direction (Oz), as $\mathbf{div}(D) = 0$, we obtain: $E_{0,z} = (\mathbb{P}^{-1}\mathcal{E}_0)_z = 0$, i.e. $\sin\varphi(\cos\theta\mathcal{E}_{0,\xi} + \sin\theta\mathcal{E}_{0,\eta}) + \cos\theta\mathcal{E}_{0,\zeta} = 0$. The

two possible polarizations of the plane wave are: $E_{0,x} = 0$ and $E_{0,y} = 0$:
• If $E_{0,x} = (\mathbb{P}^{-1}\mathcal{E}_0)_z = 0$, then $\cos\theta\mathcal{E}_{0,1} + \sin\theta\mathcal{E}_{0,\eta} = 0$, consequently $\mathcal{E}_{0,\zeta} = 0$ and the dispersion relation is

$$\frac{\omega^2}{k^2} = \frac{1}{n_o^2}.$$

• If $E_{0,y} = (\mathbb{P}^{-1}\mathcal{E}_0)_y = 0$, then $\mathcal{E}_{0,\eta} = \tan\theta\mathcal{E}_{0,\xi}$. This gives the following dispersion relation:

$$\frac{\omega^2}{k^2} = \frac{\cos^2\varphi}{n_e^2} + \frac{\sin^2\varphi}{n_o^2},$$

where n_o and n_e are the two linear indexes of the medium given by

$$\chi^{(1)}(\omega) = \begin{pmatrix} n_o^2 & 0 & 0 \\ 0 & n_o^2 & 0 \\ 0 & 0 & n_e^2 \end{pmatrix}.$$

We now consider an incident plane wave for which the polarization is defined by the relations : $\cos\theta\mathcal{E}_{0,\xi} + \sin\theta\mathcal{E}_{0,\eta} = 0$ and $\mathcal{E}_{0,\zeta} = 0$. Associated to this wave polarization, the dispersion relation is $k_f^2 = \omega_f^2 n_o^2(\omega_f)$ where the index f is used for the fundamental wave. The second harmonic wave generated by the quadratic nonlinear polarization is defined by the relation $(\mathbb{P}^{-1}\mathcal{P}^{(2)}(\mathcal{E}_0))_y = 0$, which is the second class of polarization. The dispersion relation associated with the second harmonic is then given by $k_h^2 = \omega_h^2 n_h^2(\omega_h)$, where

$$\frac{1}{n_h^2(\omega_h)} = \frac{\cos^2\varphi}{n_e^2(\omega_h)} + \frac{\sin^2\varphi}{n_o^2(\omega_h)}.$$

The index h is used for the second harmonic. The linear phase matching between the fundamental and its second harmonic, is obtained when the angle φ is equal to φ_0 given by

$$\varphi_0 = \arcsin\left(\sqrt{\frac{\frac{1}{n_o^2(\omega_f)} - \frac{1}{n_o^2(\omega_h)}}{\frac{1}{n_e^2(\omega_h)} - \frac{1}{n_o^2(\omega_h)}}}\right), \tag{2.10}$$

with $\omega_h = 2\omega_f$.

In summary, the angle φ_0 corresponds to the case where both (k_f, ω_f) and $(2k_f, 2\omega_f)$ satisfy the dispersion relation of the system. When one adds the nonlinearity, one expects the following scenario:
the laser enters the medium with wave number k_f and frequency ω_f. Quadratic effects create the second harmonic $(2k_f, 2\omega_f)$. If $\varphi \neq \varphi_0$, then this harmonic is **not** resonant and it stays small. If $\varphi = \varphi_0$ (phase-matching case), then $(2k_f, 2\omega_f)$ is resonant (it satisfies the dispersion relation) and the second harmonic will grow and reach the same size as the fundamental ones. If $\varphi \approx \varphi_0$, one expects an intermediate behavior. This scenario is in fact realistic from the physical point of view and our numerical method describes it very well (see the last section).

2.3 Asymptotic equivalent model

In practice, the computation of $\partial_t \chi^{(2)}$ is not natural and can be a source of numerical instabilities. We will propose in this section a modified model that is asymptotically equivalent to the original Maxwell-Lorentz model. In the final model the nonlinear polarization is obtained by solving ordinary differential equations. We first introduce a dimensionless form of system (2.8). Letting $t = T_{ref}\tilde{t}$, $z = z_{ref}\tilde{z}$ with $z_{ref} = cT_{ref}$, $E = E_{ref}\tilde{E}$, $\chi^{(2)} = \chi^{(2)}_{ref}\tilde{\chi}^{(2)}$ and introducing $\omega_i = \omega_{ref}\tilde{\omega}_i$ for $i = a, b$ and omitting the tildes leads to the following system:

$$\left\{\begin{array}{lllllll} \partial_t \mathcal{H} & + & \mathcal{M}\partial_z \mathcal{E} & & & = & 0, \\ \chi^{(1)}_\infty \partial_t \mathcal{E} & - & \mathcal{M}\partial_z \mathcal{H} & + & \frac{\omega_a}{\varepsilon}\mathcal{U} + \frac{\omega_b}{\varepsilon}\mathcal{V} & = & -\gamma \partial_t \chi^{(2)}(\mathcal{E}, \mathcal{E}), \\ \partial_t \mathcal{F} & & & - & \frac{\omega_a}{\varepsilon}\mathcal{U} & = & 0, \\ \partial_t \mathcal{G} & & & - & \frac{\omega_b}{\varepsilon}\mathcal{V} & = & 0, \\ \partial_t \mathcal{U} & + & \frac{\omega_a}{\varepsilon}\mathcal{F} & - & \alpha_a \frac{\omega_a}{\varepsilon}\mathcal{T}\mathcal{E} & = & 0, \\ \partial_t \mathcal{V} & + & \frac{\omega_b}{\varepsilon}\mathcal{G} & - & \alpha_b \frac{\omega_b}{\varepsilon}\mathcal{T}\mathcal{E} & = & 0, \end{array}\right. \tag{2.11}$$

where $\varepsilon = \frac{1}{T_{ref}\omega_{ref}}$ and $\gamma = E_{ref}\chi^{(2)}_{ref}$. For the applications of this paper, we have:

$$T_{ref} \sim 10^{-13}s, \quad \omega_{ref} \sim 10^{16}s^{-1}, \quad \chi^{(2)}_{ref} \sim 10^{-12} \quad \text{and} \quad E_{ref} \sim 10^9$$

in S.I. units.
Therefore $\varepsilon \sim 10^{-3}$ and $\gamma \sim 10^{-3} \sim \varepsilon$. To make the presentation more clear, we define in the sequel $\tilde{\gamma} = \frac{\gamma}{\varepsilon} \sim 1$. We introduce now profile variable as follows: we search $\mathcal{H}$, $\mathcal{E}$, $\mathcal{F}$, $\mathcal{G}$, $\mathcal{U}$, $\mathcal{V}$ under the form

$$(\mathcal{H}, \mathcal{E}, \mathcal{F}, \mathcal{G}, \mathcal{U}, \mathcal{V})(t, z) = (H, E, F, G, U, V)(t, z, \theta)_{\theta = \frac{kz - \omega t}{\varepsilon}}$$

and we look at the equations satisfied by (H, E, F, G, U, V):

$$\begin{array}{l} \partial_t H + \mathcal{M}\partial_z E + \dfrac{1}{\varepsilon}\left(-\omega\partial_\theta H + \mathcal{M}k\partial_\theta E\right) = 0, \\ \\ \chi^{(1)}_\infty \partial_t E - \mathcal{M}\partial_z H + \dfrac{1}{\varepsilon}\left(\omega_a U + \omega_b V - \omega\chi^{(1)}_\infty \partial_\theta E - \mathcal{M}k\partial_\theta H\right) = -\varepsilon\gamma\left(\partial_t - \dfrac{\omega}{\varepsilon}\partial_\theta\right)\chi^{(2)}(E, E), \\ \\ \partial_t F + \frac{1}{\varepsilon}\left(-\omega\partial_\theta F - \omega_a U\right) = 0, \\ \\ \partial_t G + \frac{1}{\varepsilon}\left(-\omega\partial_\theta G - \omega_b V\right) = 0, \\ \\ \partial_t U + \frac{1}{\varepsilon}\left(-\omega\partial_\theta U + \omega_a F - \alpha_a\omega_a \mathcal{T}E\right) = 0, \\ \\ \partial_t V + \frac{1}{\varepsilon}\left(-\omega\partial_\theta V + \omega_b G - \alpha_b\omega_b \mathcal{T}E\right) = 0. \end{array} \tag{2.12}$$

If X denotes a generic name for the variables (H, E, F, G, U, V), letting

$$X(t,x,\theta) = \sum_{m\geq 0} \varepsilon^m X_m(t,x,\theta)$$

and collecting terms of equal power of ε in (2.12) leads for the coefficient of $\frac{1}{\varepsilon}$:

$$-\partial_\theta(\omega H_0 - k\mathcal{M}E_0) = 0,$$

$$-\omega\chi_\infty^{(1)}\partial_\theta E_0 - \mathcal{M}k\partial_\theta H_0 + \omega_a U_0 + \omega_b V_0 = 0,$$

$$-\omega\partial_\theta F_0 - \omega_a U_0 = 0,$$

$$-\omega\partial_\theta G_0 - \omega_b V_0 = 0,$$

$$-\omega\partial_\theta U_0 + \omega_a F_0 - \alpha_a\omega_a\mathcal{T}E_0 = 0,$$

$$-\omega\partial_\theta V_0 + \omega_b G_0 - \alpha_b\omega_b\mathcal{T}E_0 = 0.$$

One obtains:

$$\left(-\omega^2\partial_\theta^2\chi^{(1)}(\frac{\omega\partial_\theta}{i}) + k^2\partial_\theta^2\mathcal{M}^2\right)E_0 = 0.$$

As explained in the introduction, the profile are supposed to be periodic with respect to the variable θ, and denoting $E_0 = \sum_p E_{0p}e^{ip\theta}$, one gets

$$\left(-\omega^2 p^2\chi^{(1)}(p\omega) + k^2p^2\mathcal{M}^2\right)E_{0p} = 0. \tag{2.13}$$

For $p = 1$, since $\det\left(-\omega^2\chi^{(1)}(\omega) + k^2\mathcal{M}^2\right) = 0$, one can find a non trivial E_{01}. For $p = 2$, in the case of phase matching, one obtains a nontrivial E_{02}. Otherwise, $E_{02} = 0$. Anyway, $E_{0p} = 0$ for $|p| \geq 3$.
Term of size ε^0 in (2.12) are

$$\partial_t H_0 + \mathcal{M}\partial_z E_0 + (-\omega\partial_\theta H_1 + \mathcal{M}k\partial_\theta E_1) = 0,$$

$$\chi_\infty^{(1)}\partial_t E_0 - \mathcal{M}\partial_z H_0 + \left(\omega_a U_1 + \omega_b V_1 - \omega\chi_\infty^{(1)}\partial_\theta E_1 - \mathcal{M}k\partial_\theta H_1\right) = -\gamma\left(\partial_t - \frac{\omega}{\varepsilon}\partial_\theta\right)\chi^{(2)}(E_0, E_0),$$

$$\partial_t F_0 + (-\omega\partial_\theta F_1 - \omega_a U_1) = 0,$$

$$\partial_t G_0 + (-\omega\partial_\theta G_1 - \omega_b V_1) = 0,$$

$$\partial_t U_0 + (-\omega\partial_\theta U_1 + \omega_a F_1 - \alpha_a\omega_a\mathcal{T}E_1) = 0,$$

$$\partial_t V_0 + \tfrac{1}{\varepsilon}(-\omega\partial_\theta V_1 + \omega_b G_1 - \alpha_b\omega_b\mathcal{T}E_1) = 0.$$

Therefore, the first contribution of the nonlinearity in the equation satisfied by E_0 is the term

$$\omega\gamma\partial_\theta\chi^{(2)}(E_0,E_0). \tag{2.14}$$

Now, we introduce the following semi-linear model as a substitute of (2.11):

$$\left\{\begin{array}{lllllll} \partial_t\tilde{\mathcal{H}} & + & \mathcal{M}\partial_z\tilde{\mathcal{E}} & & & = & 0,\\ \chi_\infty^{(1)}\partial_t\tilde{\mathcal{E}} & - & \mathcal{M}\partial_z\tilde{\mathcal{H}} & + & \frac{\omega_a}{\varepsilon}\tilde{\mathcal{U}}+\frac{\omega_b}{\varepsilon}\tilde{\mathcal{V}} & = & 0,\\ \partial_t\tilde{\mathcal{F}} & & & - & \frac{\omega_a}{\varepsilon}\tilde{\mathcal{U}} & = & 0,\\ \partial_t\tilde{\mathcal{G}} & & & - & \frac{\omega_b}{\varepsilon}\tilde{\mathcal{V}} & = & 0,\\ \partial_t\tilde{\mathcal{U}} & + & \frac{\omega_a}{\varepsilon}\tilde{\mathcal{F}} & - & \alpha_a\frac{\omega_a}{\varepsilon}\mathcal{T}\tilde{\mathcal{E}} & = & \omega_a\gamma J_a\chi^{(2)}(\tilde{\mathcal{E}},\tilde{\mathcal{E}}),\\ \partial_t\tilde{\mathcal{V}} & + & \frac{\omega_b}{\varepsilon}\tilde{\mathcal{G}} & - & \alpha_b\frac{\omega_b}{\varepsilon}\mathcal{T}\tilde{\mathcal{E}} & = & \omega_b\gamma J_b\chi^{(2)}(\tilde{\mathcal{E}},\tilde{\mathcal{E}}), \end{array}\right. \tag{2.15}$$

where J_a and J_b are diagonal second order tensors with constant coefficients that we will determined below in order to obtain the same effective nonlinearity as in (2.14). The corresponding set of equations associated to the profiles is:

$$\partial_t\tilde{H}+\mathcal{M}\partial_z\tilde{E}+\frac{1}{\varepsilon}\left(-\omega\partial_\theta\tilde{H}+\mathcal{M}k\partial_\theta\tilde{E}\right)=0,$$

$$\chi_\infty^{(1)}\partial_t\tilde{E}-\mathcal{M}\partial_z\tilde{H}+\frac{1}{\varepsilon}\left(\omega_a\tilde{U}+\omega_b\tilde{V}-\omega\chi_\infty^{(1)}\partial_\theta\tilde{E}-\mathcal{M}k\partial_\theta\tilde{H}\right)=0,$$

$$\partial_t\tilde{F}+\tfrac{1}{\varepsilon}\left(-\omega\partial_\theta\tilde{F}-\omega_a\tilde{U}\right)=0,$$

$$\partial_t\tilde{G}+\tfrac{1}{\varepsilon}\left(-\omega\partial_\theta\tilde{G}-\omega_b\tilde{V}\right)=0,$$

$$\partial_t\tilde{U}+\tfrac{1}{\varepsilon}\left(-\omega\partial_\theta\tilde{U}+\omega_a\tilde{F}-\alpha_a\omega_a\mathcal{T}\tilde{E}\right)=\omega_a\gamma J_a\chi^{(2)}(\tilde{E},\tilde{E}),$$

$$\partial_t V+\tfrac{1}{\varepsilon}\left(-\omega\partial_\theta\tilde{V}+\omega_b\tilde{G}-\alpha_b\omega_b\mathcal{T}\tilde{E}\right)=\omega_b\gamma J_b\chi^{(2)}(\tilde{E},\tilde{E}).$$

At order $O(\frac{1}{\varepsilon})$, the equations satisfied by the tilde variables are the same as the ones derived from the original system. We are interested now by the first nonlinear contribution in the equation satisfied by E_0. Let us write these equations at order $O(1)$:

$$\partial_t\tilde{H}_0+\mathcal{M}\partial_z\tilde{E}_0+\left(-\omega\partial_\theta\tilde{H}_1+\mathcal{M}k\partial_\theta\tilde{E}_1\right)=0, \tag{2.16}$$

$$\chi_\infty^{(1)}\partial_t\tilde{E}_0-\mathcal{M}\partial_z\tilde{H}_0+\left(\omega_a\tilde{U}_1+\omega_b\tilde{V}_1-\omega\chi_\infty^{(1)}\partial_\theta\tilde{E}_1-\mathcal{M}k\partial_\theta\tilde{H}_1\right)=0, \tag{2.17}$$

$$\partial_t\tilde{F}_0+\left(-\omega\partial_\theta\tilde{F}_1-\omega_a\tilde{U}_1\right)=0, \tag{2.18}$$

$$\partial_t\tilde{G}_0+\left(-\omega\partial_\theta\tilde{G}_1-\omega_b\tilde{V}_1\right)=0, \tag{2.19}$$

$$\partial_t \tilde{U}_0 + \left(-\omega\partial_\theta \tilde{U}_1 + \omega_a \tilde{F}_1 - \alpha_a\omega_a \mathcal{T}\tilde{E}_1\right) = \omega_a\gamma J_a \chi^{(2)}(\tilde{E},\tilde{E}), \tag{2.20}$$

$$\partial_t \tilde{V}_0 + \frac{1}{\varepsilon}\left(-\omega\partial_\theta \tilde{V}_1 + \omega_b \tilde{G}_1 - \alpha_b\omega_b \mathcal{T}\tilde{E}_1\right) = \omega_b\gamma J_b \chi^{(2)}(\tilde{E},\tilde{E}). \tag{2.21}$$

Applying $-\omega\partial_\theta$ on (2.20) and using (2.18) gives

$$\left(\omega^2\partial_\theta^2 + \omega_a^2\right)\tilde{U}_1 - \omega_a\partial_t\tilde{F}_0 + \alpha_a\omega_a\omega\mathcal{T}\partial_\theta\tilde{E}_1 - \omega\partial_t\partial_\theta\tilde{U}_0 = -\omega\omega_a\gamma J_a\partial_\theta\chi^{(2)}(\tilde{E}_0,\tilde{E}_0).$$

The same holds for $\tilde{V}_1$:

$$\left(\omega^2\partial_\theta^2 + \omega_b^2\right)\tilde{V}_1 - \omega_b\partial_t\tilde{G}_0 + \alpha_b\omega_b\omega\mathcal{T}\partial_\theta\tilde{E}_1 - \omega\partial_t\partial_\theta\tilde{V}_0 = -\omega\omega_b\gamma J_b\partial_\theta\chi^{(2)}(\tilde{E}_0,\tilde{E}_0).$$

Plugging these values of $\tilde{U}_1$ and $\tilde{V}_1$ in (2.17) gives the following nonlinear contribution in the right-hand side

$$\left[\omega\omega_a^2\gamma J_a\left(\omega^2\partial_\theta^2+\omega_a^2\right)^{-1} + \omega\omega_b^2\gamma J_b\left(\omega^2\partial_\theta^2+\omega_b^2\right)^{-1}\right]\partial_\theta\chi^{(2)}(\tilde{E}_0,\tilde{E}_0).$$

In order to have equivalent models in this asymptotic limit, we impose that this quantity is equal to (2.14), that is

$$\omega_a^2\left(\omega^2\partial_\theta^2+\omega_a^2\right)^{-1}J_a + \omega_b^2\left(\omega^2\partial_\theta^2+\omega_b^2\right)^{-1}J_b = 1. \tag{2.22}$$

There are several way to satisfy this relationship approximatively. From the practical point of view, they are all equivalent. The first solution is to allow differential operators for J_a and J_b and to solve this relationship exactly. For example, one can take

$$J_a = \alpha(1+\frac{\omega^2}{\omega_a^2}\partial_\theta^2) \text{ and } J_b = (1-\alpha)(1+\frac{\omega^2}{\omega_b^2}\partial_\theta^2).$$

Note that, with this definition of J_a and J_b, the system is not semi-linear anymore! The second solutions relies on the fact that, only at most two harmonics play a significant role: $e^{i\theta}$ and eventually $e^{2i\theta}$ in the case of phase matching. Therefore, we can impose (2.22) only on the functions $e^{i\theta}$ and $e^{2i\theta}$. In this case, one gets

$$J_a = \frac{(\omega_a^2-\omega^2)(\omega_a^2-4\omega^2)}{\omega_a^2(\omega_a^2-\omega_b^2)} \tag{2.23}$$

and

$$J_b = \frac{(\omega_b^2-\omega^2)(\omega_b^2-4\omega^2)}{\omega_b^2(\omega_b^2-\omega_a^2)}. \tag{2.24}$$

In the sequel, this solution will be adopted. Finally, the equivalent system that we consider is (omitting the tildes)

$$\left\{\begin{array}{lcllcll}
\partial_t\mathcal{H} & + & \mathcal{M}\partial_z\mathcal{E} & & & = & 0,\\
\chi_\infty^{(1)}\partial_t\mathcal{E} & - & c^2\mathcal{M}\partial_z\mathcal{H} & + & \omega_a\mathcal{U}+\omega_b\mathcal{V} & = & 0,\\
\partial_t\mathcal{F} & & & - & \omega_a\mathcal{U} & = & 0,\\
\partial_t\mathcal{G} & & & - & \omega_b\mathcal{V} & = & 0,\\
\partial_t\,\mathcal{U} & + & \omega_a\mathcal{F} & - & \alpha_a\omega_a\mathcal{T}\mathcal{E} & = & \omega_a\gamma J_a\chi^{(2)}(\mathcal{E},\mathcal{E}),\\
\partial_t\mathcal{V} & + & \omega_b\mathcal{G} & - & \alpha_b\omega_b\mathcal{T}\mathcal{E} & = & \omega_b\gamma J_b\chi^{(2)}(\mathcal{E},\mathcal{E}),
\end{array}\right.$$

with J_a and J_b respectively given by (2.23) and (2.24). Its dimensionless form is given in (2.15).

In other to put the system (2.15) in a canonical form, let us consider the following change of variables:

$$\mathcal{H}^* = \mathcal{H}, \quad \mathcal{E}^* = \sqrt{\chi_\infty^{(1)}}\mathcal{E}, \quad \mathcal{U}^* = \left(\sqrt{\alpha_1 \mathcal{T}}\right)^{-1} \mathcal{U},$$

$$\mathcal{V}^* = \left(\sqrt{\alpha_2 \mathcal{T}}\right)^{-1} \mathcal{V}, \quad \mathcal{F}^* = \left(\sqrt{\alpha_1 \mathcal{T}}\right)^{-1} \mathcal{F}, \quad \mathcal{G}^* = \left(\sqrt{\alpha_2 \mathcal{T}}\right)^{-1} \mathcal{G}.$$

Then let us define a variable u by:

$$u = (\mathcal{H}^*, \mathcal{E}^*, \mathcal{F}^*, \mathcal{G}^*, \mathcal{U}^*, \mathcal{V}^*)^T.$$

The non-dimensional Maxwell's system take the form:

$$\partial_t u + A\partial_z u + \frac{1}{\varepsilon} L_0 u = f(u), \tag{2.25}$$

where A is a symmetric real matrix, L_0 is skew symmetric matrix and $f(u)$ is a quadratic function. The form (2.25) is generic and we now propose a systematic numerical strategy for systems of this form.

3 Presentation of the method and semi-discretization in time.

3.1 The singular equation.

The aim of this section is to recall some tools of geometrical optics developed during the last decade by J.-L. Joly, G. Métivier and J. Rauch (see [15, 16] for example). Let us consider the following system of PDE's:

$$\left(\partial_t + \sum_{j=1}^{n} A_j \partial_{x_j} + \frac{1}{\varepsilon} L_0\right) u^\varepsilon = f(u^\varepsilon), \tag{3.26}$$

where $u^\varepsilon : [0,T] \times \mathbb{R}^n \to \mathbb{R}^p$. The matrices A_j are symmetric real, L_0 is skew symmetric. f is a smooth nonlinear function defined on $\mathbb{R}^p$ and $\varepsilon > 0$ is a small real parameter. The main goal of geometrical optics is to construct oscillatory solutions to (3.26), when $\varepsilon \to 0$, under the form:

$$u^\varepsilon(t,x) = \varepsilon^\alpha \left(e^{i\frac{k\cdot x - \omega t}{\varepsilon}} a(t,x) + c.c.\right) + o(\varepsilon^\alpha), \tag{3.27}$$

where $k \in \mathbb{R}^n$ is the wave vector, ω the pulsation and $\alpha \in \mathbb{R}^+$. The following ingredients and notations will be useful for the analysis. For $\xi = (\xi_1, \cdots, \xi_n) \in \mathbb{R}^n$, we denote by

$$A(\xi) = \sum_{j=1}^{n} A_j \xi_j.$$

The matrix $iA(\xi) + L_0$ is skew-adjoint and we denote by $i\lambda_l(\xi) \in i\mathbb{R}$ its eigenvalues and by $\Pi_l(\xi)$ the orthogonal projector on the kernel of $iA(\xi) + L_0 - i\lambda_l(\xi)$. The characteristic variety of the operator $\partial_t + A(\partial_x) + \dfrac{L_0}{\varepsilon}$ is the set defined by

$$\{(\xi, \lambda_l(\xi))/ \quad \xi \in \mathbb{R}^n, \quad l = 1 \text{ to } k\}.$$

It is an algebraic variety.
Finally, denote by $Q_l(\xi)$ the partial inverse of $-i\lambda_l(\xi) + iA(\xi) + L_0$ such that

$$(-i\lambda_l(\xi) + iA(\xi) + L_0)\, Q_l(\xi) = 1 - \Pi_l(\xi) = Q_l(\xi)\, (-i\lambda_l(\xi) + iA(\xi) + L_0).$$

Now plugging (3.27) in (3.26), the terms of size $\varepsilon^{\alpha-1}$ give:

$$(-i\omega + iA(k) + L_0)a = 0. \tag{3.28}$$

Equation (3.28) has a non-zero solution if and only if there exists l_0 such that $\omega = \lambda_{l_0}(k)$. From now one, we take $k \in \mathbb{R}^n$ and $\omega = \lambda_{l_0}(k)$ such that

$$\text{the multiplicity of the eigenvalue } \lambda_{l_0}(k) \text{ is constant in a neighborhood of } k. \tag{3.29}$$

This implies that $\xi \mapsto \Pi_{l_0}(\xi)$, $\xi \mapsto \lambda_{l_0}(\xi)$ and $\xi \mapsto Q_{l_0}(\xi)$ are smooth functions in the neighborhood of $\xi = k$.
The time interval on which we describe the evolution of the solution can be of length $O(1)$ or $O(\dfrac{1}{\varepsilon})$. Time scales of size $O(1)$ are the geometrical optics time scales and time of size $O(\dfrac{1}{\varepsilon})$ are the diffractive time scales since on such time interval, diffraction's effects play a fundamental role. In both cases, the parameter α which determines the size of the solution in (3.27) has to be chosen such that the nonlinear effects occur at the correct time. It depends on the nonlinearity of the system (*i.e.* on function f). If $f(u) \sim u^p$ $(p > 0)$ as $u \to 0$, then a solution of (3.26) of size ε^α as a lifetime of size (at least) $\varepsilon^{\alpha(p-1)}$. Therefore, for geometrical optics time scale, one has $\alpha = 0$ and for diffractive time scale $\alpha = \dfrac{1}{p-1}$. One of the main tools introduced by Joly, Métivier and Rauch is the systematic use of the *singular equation*. We now precise this method. One wants to find solution $u^\varepsilon(t, x)$ of (3.26) under the form:

$$u^\varepsilon(t, x) = \mathcal{U}^\varepsilon(\frac{k \cdot x - \omega t}{\varepsilon}, t, x) \tag{3.30}$$

where the function $\mathcal{U}^\varepsilon(\theta,t,x)$ is periodic in the θ variable. Of course, the function $\mathcal{U}^\varepsilon$ is not well defined. In order to have a precise definition of it, the idea is to write the following equation for $\mathcal{U}^\varepsilon$:

$$\partial_t \mathcal{U}^\varepsilon + A(\partial_x)\mathcal{U}^\varepsilon + \frac{1}{\varepsilon}\mathcal{L}(\partial_\theta)\mathcal{U}^\varepsilon = f(\mathcal{U}^\varepsilon) \tag{3.31}$$

where

$$\mathcal{L}(\partial_\theta) = -\omega\partial_\theta + A(k)\partial_\theta + L_0.$$

This equation is *a priori* satisfied for all t,x and only for $\theta = \dfrac{k\cdot x - \omega t}{\varepsilon}$. The main point is then to impose that (3.31) is satisfied by $\mathcal{U}^\varepsilon$ for all t,x but also **for any** θ. It is clear that:

Proposition 3.1. *If $\mathcal{U}^\varepsilon$ is solution to (3.31) for $(\theta,t,x)\in[0,2\pi]\times[0,T]\times\mathbb{R}^n$ then u^ε defined by (3.30) is solution to (3.26) for $(t,x)\in[0,T]\times\mathbb{R}^n$.*

Therefore, we will focus on the analysis and the approximation of (3.31). Thanks to proposition 3.1, all these results will be translated in terms of u^ε.

3.2 Nonlinear geometrical optics.

One use the WKB techniques in order to construct the desired approximate solution. If one plugs in the system the plane wave $e^{i\theta}$ then higher harmonics $e^{ip\theta}$ for $p\in\mathbb{Z}$ will be created by nonlinear effects. Some of these harmonics will be resonant in the sense that $(pk,p\omega)$ can be in the characteristic variety. We denote by R the resonant set defined by

$$\mathcal{R} = \Big\{ p\in\mathbb{Z} \quad \text{such that} \quad (pk,p\omega) \text{ is in the characteristic variety} \Big\}.$$

As in [11], we assume that $\mathcal{R}$ is a finite set.
As soon as a physical system has a nonlinear dispersion relation, this assumption is satisfied, see [19] for explicit computations. Note that $\{1,-1\}\in\mathcal{R}$. When $0\in\mathcal{R}$, the physical phenomena that appears is the rectification effect and when $\{2,-2\}\in\mathcal{R}$, the corresponding physical phenomena is the phase matching. We seek for an approximate solution of the form:

$$\mathcal{U}^a_\varepsilon(\theta,t,x) = \mathcal{U}_0(\theta,t,x) + \varepsilon\mathcal{U}_1(\theta,t,x).$$

For the simplicity of the analysis, we assume from now one that f is a quadratic mapping denoted by

$$f(u) = f(u,u),$$

where f is bilinear symmetric.
At order $O\left(\frac{1}{\varepsilon}\right)$, one gets: $\mathcal{L}(\partial_\theta)\mathcal{U}_0 = 0$. Expanding $\mathcal{U}_0$ in Fourier series yields

$$\mathcal{U}_0 = \sum_{p\in\mathbb{Z}} \mathcal{U}_{0,p} e^{ip\theta}$$

and

$$\mathcal{L}(ip)\mathcal{U}_{0,p} = 0. \tag{3.32}$$

For $p \notin \mathcal{R}$ equation (3.32) gives

$$\mathcal{U}_{0,p} = 0 \tag{3.33}$$

while when $p \in \mathcal{R}$

$$\mathcal{U}_{0,p} = \Pi(pk)\mathcal{U}_{0,p}. \tag{3.34}$$

At order $O(1)$ one obtains:

$$\mathcal{L}(\partial_\theta)\mathcal{U}_1 + (\partial_t + A(\partial_x))\mathcal{U}_0 = f(\mathcal{U}_0, \mathcal{U}_0).$$

Expanding in Fourier series yields:

$$\mathcal{L}(ip)\mathcal{U}_{1,p} + (\partial_t + A(\partial_x))\mathcal{U}_{0,p} = \sum_{p_1+p_2=p} f(\mathcal{U}_{0,p_1}, \mathcal{U}_{0,p_2}). \tag{3.35}$$

For $p \notin \mathcal{R}$, since $\mathcal{L}(ip)$ is one-to-one, (3.35) gives

$$\mathcal{U}_{1,p} = \mathcal{L}(ip)^{-1} \sum_{p_1+p_2=p} f(\mathcal{U}_{0,p_1}, \mathcal{U}_{0,p_2}), \tag{3.36}$$

since $\mathcal{U}_{0,p} = 0$ for $p \notin \mathcal{R}$.
For $p \in \mathcal{R}$, the matrix $\mathcal{L}(ip)$ is not one-to-one, therefore, a necessary and sufficient condition for (3.35) to have a solution is that

$$-(\partial_t + A(\partial_x))\mathcal{U}_{0,p} + \sum_{p_1+p_2=p} f(\mathcal{U}_{0,p_1}, \mathcal{U}_{0,p_2})$$

is in the range of $\mathcal{L}(ip)$. This condition can be written as:

$$(\partial_t + \Pi(pk)A(\partial_x)\Pi(pk))\mathcal{U}_{0,p} = \sum_{\substack{p_1+p_2=p,\\ p_1\in\mathcal{R},\ p_2\in\mathcal{R}}} \Pi(pk) f(\mathcal{U}_{0,p_1}, \mathcal{U}_{0,p_2}). \tag{3.37}$$

One still have to characterize the operator $\Pi(pk)A(\partial_x)\Pi(pk)$.

Lemma 3.1. *If $(pk, p\omega)$ is a regular point of the characteristic variety then $\Pi(pk)A(\partial_x)\Pi(pk) = \lambda'(pk)\cdot\partial_x\Pi(pk)$ where $\xi \mapsto \lambda(\xi)$ is the branch of the characteristic variety for which $\lambda(pk) = p\omega$.*

However for $p = 0$, $(0,0)$ is never (in physical application) a regular point. One needs the following result due to Lannes [19].

Lemma 3.2. *If $(0,0)$ is an isolated singular point of the characteristic variety of $\mathcal{L} := \partial_t + A(\partial_x) + \dfrac{L_0}{\varepsilon}$ then the characteristic variety of $\Pi(0)\partial_t + \Pi(0)A(\partial_x)\Pi(0)$ is the tangent cone of the characteristic variety of $\mathcal{L}$ at $(0,0)$.*

This means that in this case, the operator $\Pi(0)A(\partial_x)\Pi(0)$ is not scalar anymore. One can think for example to a Maxwell-type system or to a system corresponding to the wave equation.
Therefore, the set of equation (3.37) reduces to a finite set of transport equations (for $p \neq 0$) and eventually a Maxwell-type system.
Two particular cases are important for applications:

when $\mathcal{R} = \{-1, +1\}$: there are no rectification effects, no phase matching. The evolution equation is linear:

$$\big(\partial_t + \lambda_{l_0}'(k) \cdot \partial_x\big)\, \mathcal{U}_{0,1} = 0.$$

when $\mathcal{R} = \{-1, +1, -2, +2\}$: there is no rectification effects, but the phase matching exists. On obtain a set of coupled transport equations:

$$\big(\partial_t + \lambda_{l_0}'(k) \cdot \partial_x\big)\, \mathcal{U}_{0,1} = 2\Pi(k) f(\mathcal{U}_{0,2}, \bar{\mathcal{U}}_{0,1}),$$

$$\big(\partial_t + \lambda'(2k) \cdot \partial_x\big)\, \mathcal{U}_{0,2} = \Pi(2k) f(\mathcal{U}_{0,1}, \mathcal{U}_{0,1}).$$

In any case, one can solve equation (3.37) on a time interval $[0,T]$ for sufficiently regular initial data.

Proposition 3.2. *Let $a_p \in H_x^s(\mathbb{R}^n)$ for $s > n/2$ be given functions and $p \in \mathcal{R}$. There exists $T > 0$ and an unique solution $\mathcal{U}_{0,p}(t,x) \in \mathcal{C}([0,T]; H_x^s(\mathbb{R}^n))$ to (3.37) such that $\mathcal{U}_{0,p}(0,x) = a_p(x)$.*

Once $\mathcal{U}_{0,p}$ has been determined, then $\mathcal{U}_{1,p}$ is given by (3.36) for $p \notin \mathcal{R}$ and

$$(1 - \Pi(pk))\mathcal{U}_{1,p} = Q(pk) \left(- (\partial_t + A(\partial_x))\, \mathcal{U}_{0,p} - \sum_{\substack{p_1 + p_2 = p, \\ p_1 \in \mathcal{R}, \quad p_2 \in \mathcal{R}}} f(\mathcal{U}_{0,p_1}, \mathcal{U}_{0,p_2}) \right). \tag{3.38}$$

It follows that

$$\mathcal{U}_\varepsilon^a := \sum_{p \in \mathcal{R}} \mathcal{U}_{0,p} e^{ip\theta} + \varepsilon \sum_{p \in \mathcal{R}} \mathcal{U}_{1,p} e^{ip\theta}$$

satisfies

$$\left(\partial_t + A(\partial_x) + \frac{1}{\varepsilon}\mathcal{L}(\partial_\theta)\right)\mathcal{U}_\varepsilon^a - f(\mathcal{U}_\varepsilon^a,\mathcal{U}_\varepsilon^a) = O(\varepsilon) \text{ on } [0,T].$$

For higher order terms, one can (as usual) build a whole expansion at any order of ε writing:

$$\mathcal{U}^\varepsilon(\theta,t,x) = \sum_{m=0}^{M} \mathcal{U}_m(\theta,t,x)\varepsilon^m + O(\varepsilon^{M+1}).$$

0ne gets at order ε^{m-1}:

$$(\partial_t + A(\partial_x))\,\mathcal{U}_{m-1} + \mathcal{L}(\partial_\theta)\mathcal{U}_m = \sum_{l_1+l_2=m-1} f(\mathcal{U}_{l_1},\mathcal{U}_{l_2}). \tag{3.39}$$

Expanding the unknowns in Fourier series yields

$$(\partial_t + A(\partial_x))\,\mathcal{U}_{m-1,p} + \mathcal{L}(ip)\mathcal{U}_{m,p} = \sum_{l_1+l_2=m-1}\ \sum_{p_1+p_2=p} f(\mathcal{U}_{l_1,p_1},\mathcal{U}_{l_2,p_2}). \tag{3.40}$$

Suppose that are known the $\mathcal{U}_{j,p}$ for $j \leq m-2$, $\mathcal{U}_{m-1,p}$ for $p \notin \mathcal{R}$ and $(1-\Pi(pk))\mathcal{U}_{m-1,p}$ for $p \in \mathcal{R}$.

For $p \notin \mathcal{R}$, equation (3.30) gives $\mathcal{U}_{m,p}$ in terms of the known functions since $\mathcal{L}(ip)$ is one-to-one and

$$\mathcal{U}_{m,p} = \mathcal{L}(ip)^{-1}\left(-(\partial_t + A(\partial_x))\,\mathcal{U}_{m-1,p} + \sum_{l_1+l_2=m-1}\ \sum_{p_1+p_2=p} f(\mathcal{U}_{l_1,p_1},\mathcal{U}_{l_2,p_2})\right). \tag{3.41}$$

For $p \in \mathcal{R}$, a necessary condition for (3.40) to have a solution is

$$(\partial_t + \Pi(pk)A(\partial_x)\Pi(pk))\mathcal{U}_{m-1,p} = \sum_{l_1+l_2=m-1}\ \sum_{p_1+p_2=p} \Pi(pk) f(\mathcal{U}_{l_1,p_1},\mathcal{U}_{l_2,p_2}), \tag{3.42}$$

which is a **linear** system on $(\mathcal{U}_{m-1,p}))_{p\in\mathcal{R}}$ with a source term. One therefore has:

Proposition 3.3. *For all $(\Pi(pk)a_p^{m-1}) \in H_x^s(\mathbb{R}^n)$, $p \in \mathcal{R}$, there exists a unique $\Pi(pk)\mathcal{U}_p^{m-1}$ solution to (3.42) such that $\Pi(pk)\mathcal{U}_p^{m-1}(0,x) = \Pi(pk)a_p^{m-1}(x)$.*

Note that the time T is the same than in the previous proposition. Once functions $\Pi(pk)\mathcal{U}_p^{m-1}$ are known, one deduces from (3.40):

$$\Big(1-\Pi(pk)\Big)\,\mathcal{U}_{m,p} = Q(pk)\left(-(\partial_t + A(\partial_x))\,\mathcal{U}_{m-1,p} + \sum_{l_1+l_2=m-1}\ \sum_{p_1+p_2=p} f(\mathcal{U}_{l_1,p_1},\mathcal{U}_{l_2,p_2})\right). \tag{3.43}$$

Let $P = max(\mathcal{R})$. We therefore have proved:

Proposition 3.4. *For $m = 0, \cdots, M$ and $p \in \mathcal{R}$, let $(a_p^m) \in H_x^\infty(\mathbb{R}^n)$ such that $\Pi(pk)a_{m,p} = a_{m,p}$. Then, for $p \in \mathbb{Z}$ and $m = 0, \cdots, M$, there exist some functions $(\mathcal{U}_{m,p}) \in \mathcal{C}([0,T]; H_x^s(\mathbb{R}^n))$ such that:*

- $\mathcal{U}_{0,p} \equiv 0$ *if* $p \notin \mathcal{R}$.
- $\mathcal{U}_{m,p} \equiv 0$ *if* $|p| > P(m+1)$.
- $\mathcal{U}_{0,p}(0,x) = a_p^0$, $p \in \mathcal{R}$ *and* $(\mathcal{U}_p^0)_{p\in\mathcal{R}}$ *is the unique solution to (3.37).*
- $(\mathcal{U}_{m,p})_{p\notin\mathcal{R}}$ *and* $((1-\Pi(pk))\mathcal{U}_{m,p})_{p\in\mathcal{R}}$ *are given respectively by (3.41) and (3.43).*
- $(\Pi(pk)\mathcal{U}_{m,p})_{p\in\mathcal{R}}$ *satisfy* $\Pi(pk)\mathcal{U}_{m,p}(0,x) = a_{m,p}(x)$ *and is the only solution to (3.42) in* $\mathcal{C}([0,T]; H_x^s(\mathbb{R}^n))$.

Then

$$\mathcal{U}_{\varepsilon,M}^a(\theta,t,x) = \sum_{m=0}^{M} \varepsilon^m \sum_{p\in\mathbb{Z}} e^{ip\theta}\mathcal{U}_{m,p}(t,x)$$

satisfies

$$(\partial_t + A(\partial_x) + \frac{1}{\varepsilon}\mathcal{L}(\partial_\theta))\mathcal{U}_{\varepsilon,M}^a - f(\mathcal{U}_{\varepsilon,M}^a, \mathcal{U}_{\varepsilon,M}^a) = O(\varepsilon^M)$$

in $L^\infty(0,T;H^s)$ norm for all s.

Remark 3.1. *The only initial data that one can prescribe are that of $\Pi(pk)\mathcal{U}_{m,p}$ for $p \in \mathcal{R}$.*

We now give an error estimate for this expansion:

Proposition 3.5. *Let $\mathcal{U}_\varepsilon^0(\theta,x) = \mathcal{U}_{\varepsilon,M}^a(\theta,0,x)$. There exists a unique solution $\mathcal{U}^\varepsilon(\theta,t,x)$ solution to (3.31) in $\mathcal{C}([0,T],H^s)$ such that $\mathcal{U}^\varepsilon(\theta,0,x) = \mathcal{U}_\varepsilon^0(\theta,x)$ and*

$$\left|\mathcal{U}^\varepsilon(\theta,t,x) - \mathcal{U}_{\varepsilon,M}^a\right|_{L^\infty(0,T;H^s_{\theta,x}([0,2\pi]\times\mathbb{R}^n))} \leq C\varepsilon^M.$$

Proof.
Take $\mathcal{V}^\varepsilon = \mathcal{U}^\varepsilon - \mathcal{U}_{\varepsilon,M}^a$. Then $\mathcal{V}^\varepsilon$ satisfies:

$$(\partial_t + A(\partial_x) + \frac{1}{\varepsilon}\mathcal{L}(\partial_\theta))\mathcal{V}^\varepsilon = O(\varepsilon^M) + 2f(\mathcal{V}^\varepsilon, \mathcal{U}_{\varepsilon,M}^a) + f(\mathcal{V}^\varepsilon,\mathcal{V}^\varepsilon),$$

with

$$\mathcal{V}^\varepsilon(\theta,0,x) = 0.$$

One then makes standard energy estimates. The crucial point is that the operator $\mathcal{L}(\partial_\theta)$ is skew-adjoint (see [8] for non skew-adjoint cases).

■

3.3 Semi-discretization in time.

In order to compute solution to (3.26), we discretized in fact equation (3.31). The important part of this discretization is to keep the fundamental property that the linear part generates a unitary group on H^s. We have to deal with two different truncation errors. The first one concerns the time discretization and is classical. The second one is related to the phase variable θ. We will show below that in order to obtain an error of order ε^{M_1}, it is sufficient to project the solution onto the linear space spanned by

$$\{e^{ip\theta}, \quad -P_1 \leq p \leq P_1\},$$

where the integer P_1 is such that $P_1 = P(M_1+1)$. Recall that P is the maximum of the resonant set $\mathcal{R}$. Moreover we call Π_{P_1} the orthogonal projection in $L^2([0,2\pi])$ onto this linear space.

The discretization that one considers is:

$$\frac{\mathcal{U}^{n+1}-\mathcal{U}^n}{\delta t} + \left(A(\partial_x) + \frac{1}{\varepsilon}\mathcal{L}(\partial_\theta)\right)\frac{\mathcal{U}^{n+1}+\mathcal{U}^n}{2} = \Pi_{P_1} f(\mathcal{U}^n,\mathcal{U}^n), \tag{3.44}$$

with

$$\mathcal{U}^0(\theta,x) = \mathcal{U}^a_{\varepsilon,M_1}(\theta,0,x).$$

We denote by $\mathcal{U}^n(\theta,x)$ the approximate value, computed from (3.44), of the solution to (3.31) at time $n\delta t$ and at point θ, x. Note that the nonlinear term is discretized explicitly. The initial data is that given by the formal expansion obtained in the previous section. The aim of this section is to prove:

Theorem 3.1. *There exists $\eta_0 > 0$ and $\varepsilon_0 > 0$, $C_p > 0$, $T > 0$ such that the solution $\mathcal{U}^n$ to (3.44) satisfies if $\varepsilon \leq \varepsilon_0$ and $\delta t \leq \eta_0$:*

$$\sup_{n=0 \text{ to } [\frac{T}{\delta t}]} |\mathcal{U}^n(\theta,x) - \mathcal{U}^\varepsilon(\theta,n\delta t,x)|_{H^s_{\theta,x}([0,2\pi]\times\mathbb{R}^n)} \leq C_p(\delta t + \varepsilon^{M_1}),$$

where $\mathcal{U}^\varepsilon$ is the solution to (3.31) with initial data $\mathcal{U}^a_{\varepsilon,M_1}(\theta,0,x)$ and $\mathcal{U}^n(\theta,x)$ denotes the approximate solution at time $n\delta t$.

Proof.

• First step: we make a WKB expansion on (3.44). Just as in the previous section, one writes an approximate solution under the form:

$$\mathcal{U}^n(\theta,x) = \sum_{m=0}^{M_1} \varepsilon^m \mathcal{U}^n_m(\theta,x) + O(\varepsilon^{M_1+1}).$$

At order $O(\varepsilon^{m-1})$, one obtains the following equation which is the discrete equivalent of (3.39):

$$\frac{\mathcal{U}_{m-1}^{n+1}-\mathcal{U}_{m-1}^{n}}{\delta t}+A(\partial_x)\frac{\mathcal{U}_{m-1}^{n+1}+\mathcal{U}_{m-1}^{n}}{2}+\mathcal{L}(\partial_\theta)\frac{\mathcal{U}_{m}^{n+1}+\mathcal{U}_{m}^{n}}{2} = \sum_{l_1+l_2=m-1} f(\mathcal{U}_{l_1}^{n},\mathcal{U}_{l_2}^{n}). \tag{3.45}$$

Expanding in Fourier series yields:

$$\mathcal{U}_m^n(\theta,x)=\sum_{p\in\mathbb{Z}}\mathcal{U}_{m,p}^n(x)e^{ip\theta} \text{ with}$$

$$\begin{aligned}&\frac{\mathcal{U}_{m-1,p}^{n+1}-\mathcal{U}_{m-1,p}^{n}}{\delta t}+A(\partial_x)\frac{\mathcal{U}_{m-1,p}^{n+1}+\mathcal{U}_{m-1,p}^{n}}{2}\\ +\mathcal{L}(ip)\frac{\mathcal{U}_{m,p}^{n+1}+\mathcal{U}_{m,p}^{n}}{2} &= \sum_{l_1+l_2=m-1}\ \sum_{p_1+p_2=p} f(\mathcal{U}_{l_1,p_1}^{n},\mathcal{U}_{l_2,p_2}^{n}).\end{aligned} \tag{3.46}$$

We first investigate the case $m=0$. Equation (3.46) gives:

$$\mathcal{L}(ip)\frac{\mathcal{U}_{0,p}^{n+1}+\mathcal{U}_{0,p}^{n}}{2}=0. \tag{3.47}$$

If $p\notin\mathcal{R}$, this implies $\mathcal{U}_{0,p}^{n+1}+\mathcal{U}_{0,p}^{n}=0$ and since $\mathcal{U}_{0,p}^{n=0}=0$, one has

$$\mathcal{U}_{0,p}^{n}=0 \quad \forall n.$$

If $p\in\mathcal{R}$, this implies $\Pi(pk)\left(\mathcal{U}_{0,p}^{n+1}+\mathcal{U}_{0,p}^{n}\right)=\mathcal{U}_{0,p}^{n+1}+\mathcal{U}_{0,p}^{n}$ and since $\Pi(pk)\mathcal{U}_{0,p}^{n=0}=\mathcal{U}_{0,p}^{n=0}$, one has

$$\Pi(pk)\mathcal{U}_{0,p}^{n}=\mathcal{U}_{0,p}^{n} \quad \forall n, \tag{3.48}$$

which is the equivalent of the polarization condition (3.34).
For the case $m=1$:
If $p\notin\mathcal{R}$, we have already proved in this case that $\mathcal{U}_{0,p}^{n}=0 \quad \forall n$. Therefore one gets:

$$\frac{\mathcal{U}_{1,p}^{n+1}+\mathcal{U}_{1,p}^{n}}{2}=\mathcal{L}(ip)^{-1}\sum_{p_1+p_2=p} f(\mathcal{U}_{0,p_1}^{n},\mathcal{U}_{0,p_2}^{n}). \tag{3.49}$$

If $p\in\mathcal{R}$, (3.46) has a solution if and only if

$$\begin{aligned}&\frac{\mathcal{U}_{0,p}^{n+1}-\mathcal{U}_{0,p}^{n}}{\delta t}+\Pi(pk)A(\partial_x)\Pi(pk)\frac{\mathcal{U}_{0,p}^{n+1}+\mathcal{U}_{0,p}^{n}}{2}\\ &\qquad=\sum_{p_1+p_2=p}\Pi(pk)f(\mathcal{U}_{0,p_1}^{n},\mathcal{U}_{0,p_2}^{n}).\end{aligned} \tag{3.50}$$

Then one gets

$$\begin{aligned}&(1-\Pi(pk))\,\frac{\mathcal{U}_{1,p}^{n+1}+\mathcal{U}_{1,p}^{n}}{2}\\ &=Q(pk)\left(-\frac{\mathcal{U}_{0,p}^{n+1}-\mathcal{U}_{0,p}^{n}}{\delta t}-A(\partial_x)\frac{\mathcal{U}_{0,p}^{n+1}+\mathcal{U}_{0,p}^{n}}{2}+\sum_{p_1+p_2=p}f(\mathcal{U}_{0,p_1}^{n},\mathcal{U}_{0,p_2}^{n})\right).\end{aligned}\tag{3.51}$$

We now show how to solve the system formed by (3.50) and (3.51). We start by the resolution of (3.50). Let $\mathcal{A}_{\delta t}(\partial_x)$ the operator defined by:

$$\mathcal{A}_{\delta t}(\partial_x)=\left(1+\frac{\delta t}{2}\Pi(pk)A(\partial_x)\Pi(pk)\right)^{-1}\left(1-\frac{\delta t}{2}\Pi(pk)A(\partial_x)\Pi(pk)\right).$$

This operator acts continuously on any Sobolev space H^s and is unitary on such spaces. Equation (3.50) can be rewritten

$$\begin{aligned}\mathcal{U}_{0,p}^{n}=\mathcal{A}_{\delta t}(\partial_x)^n\mathcal{U}_{0,p}^{0}+\left(1+\frac{\delta t}{2}\Pi(pk)A(\partial_x)\Pi(pk)\right)^{-1}\times\\ \delta t\sum_{l=0}^{n}\mathcal{A}_{\delta t}(\partial_x)^{n-l}\Pi(pk)\sum_{p_1+p_2=p}f(\mathcal{U}_{0,p_1}^{l},\mathcal{U}_{0,p_2}^{l})).\end{aligned}\tag{3.52}$$

This system can be solved by a fixed point procedure (independently of δt provided that δt is small enough) and one find a solution for $n=0,\cdots,\left[\frac{T}{\delta t}\right]$.

Proposition 3.6. *There exists $\eta_0>0$ and $T>0$ such that if $\delta t\leq\eta_0$, there exists a unique sequence $\left(\mathcal{U}_{0,p}^{n}\right)_{n=0,\cdots,\left[\frac{T}{\delta t}\right]}$, $p\in\mathcal{R}$ solution to (3.52) and (3.50). Moreover, if $\mathcal{U}_{0,p}^{0}\in H^{\infty}_{\theta,x}([0,2\pi]\times\mathbb{R}^n)$ then for any $s\in\mathbb{R}$ there exists a constant $C_s>0$ such that:*

$$\sup_{n=0,\cdots,\left[\frac{T}{\delta t}\right]}\left|\mathcal{U}_{0,p}^{n}-\mathcal{U}_{0,p}(n\delta t)\right|_{H^s_{\theta,x}([0,2\pi]\times\mathbb{R}^n)}\leq C_s\delta t,$$

where $\mathcal{U}_{0,p}$ is the solution to (3.37).

Since the nonlinearity is discretized explicitly, this scheme is of order 1 even if the discretization of the linear part is of order 2. The proof of this convergence result is classical. See [7] for similar proofs in the context of wave or Schrödinger type equations.

Remark 3.2. *This proposition proves that the scheme is asymptotic preserving, that it that the limit when $\varepsilon\to 0$ of the discretization is the discretization of the limit.*

We now solve (3.49) and (3.51). The only difference with the continuous case is that one has to solve equations on sequences under the form

$$\frac{a^{n+1}+a^n}{2} = f^n. \tag{3.53}$$

Writing (3.53) at index $n-1$ yields

$$\frac{a^n+a^{n-1}}{2} = f^{n-1}.$$

and subtracting from (3.53) gives

$$a^{n+1} - a^{n-1} = 2(f^n - f^{n-1}),$$

that is

$$a^{2n} = a^0 + 2\delta t \sum_{l=1}^{n} \frac{f^{2l} - f^{2l-1}}{\delta t}$$

and a similar formula for a^{2n+1}. The following proposition follows.

Proposition 3.7. *For any solution to (3.53) one has*

$$\sup_{n=0\cdots[\frac{T}{\delta t}]} |a^n|_{H^s_x(\mathbb{R}^n)} \leq C\delta t \sum_{l=1}^{n} \left| \frac{f^l - f^{l-1}}{\delta t} \right|_{H^s_x(\mathbb{R}^n)},$$

where C does not depend on δt.

Applying this proposition to (3.49) and (3.51) and using the fact that $\dfrac{\mathcal{U}^{n+1}_{0,p} - \mathcal{U}^n_{0,p}}{\delta t}$ is given in terms of $\left(\mathcal{U}^n_{0,p}\right)$ thanks to (3.50), for $p \notin \mathcal{R}$, one gets that

$$\sup_{n=0,\cdots,[\frac{T}{\delta t}]} |\mathcal{U}^n_{1,p}|_{H^s_x} \leq C(T, |\mathcal{U}_0|_{H^s_x})$$

and for $p \in \mathcal{R}$:

$$\sup_{n=0,\cdots,[\frac{T}{\delta t}]} |(1-\Pi(pk))\mathcal{U}^n_{1,p}|_{H^s_x} \leq C(T, |\mathcal{U}_0|_{H^s_x}),$$

where the constant $C(T, |\mathcal{U}_0|_{H^s})$ does not depend on δt. It is then clear using proposition 3.6 and the expression of $\dfrac{\mathcal{U}^{n+1}_{0,p} - \mathcal{U}^n_{0,p}}{\delta t}$ in terms of $(\mathcal{U}^n_{0,p})$ that

Lemma 3.3. *Under the hypotheses of proposition 3.6, for $p \notin \mathcal{R}$, one has*

$$\sup_{n=0,\cdots,[\frac{T}{\delta t}]} |\mathcal{U}^n_{1,p}(x) - \mathcal{U}_{1,p}(n\delta t, x)|_{H^s_x} \leq C\delta t$$

and for $p \in \mathcal{R}$

$$\sup_{n=0\cdots\left[\frac{T}{\delta t}\right]} |(1-\Pi(pk))\mathcal{U}_{1,p}^n(x) - \mathcal{U}_{1,p}(n\delta t, x)|_{H_x^s} \leq C\delta t$$

where $\mathcal{U}_{1,p}$ *is the first corrector in the asymptotic expansion given in proposition 3.4.*

Remark 3.3. *This lemma shows that the first corrector when* $\varepsilon \to 0$ *of the discretization is the discretization of the first corrector.*

For $m \geq 2$, similar manipulations can be handled and one gets that:

Proposition 3.8. *The system (3.46) can be solved for* $m = 0$ *to* $M_1 - 1$ *and one constructs*

$$\mathcal{U}^n = \sum_{m=0}^{M_1} \varepsilon^m \mathcal{U}_m^n(\theta, x) + O(\varepsilon^{M_1+1}).$$

Moreover $(\mathcal{U}^n)_{n=0,\cdots,\left[\frac{T}{\delta t}\right]}$ *satisfies*

$$\sup_{n=0,\cdots,\left[\frac{T}{\delta t}\right]} \left|\mathcal{U}^n(\theta,x) - \mathcal{U}_{\varepsilon,M_1}^a(\theta, n\delta t, x)\right|_{H^s_{\theta,x}([0,2\pi]\times\mathbb{R}^n)} \leq C\delta t$$

and

$$\sup_{n=0,\cdots,\left[\frac{T}{\delta t}\right]} \left|\mathcal{U}_{\varepsilon,M_1}^a(\theta, n\delta t, x) - \mathcal{U}^\varepsilon(\theta, n\delta t, x)\right|_{H^s_{\theta,x}([0,2\pi]\times\mathbb{R}^n)} = O(\varepsilon^{M_1}),$$

where $\mathcal{U}_{\varepsilon,M_1}^a$ *is the approximate solution given by the WKB expansion in the continuous case.*

This proposition proves that one can build a WKB approximation to the discrete solution and that this discrete WKB solution is a discretization of the continuous ones. This leads to the proof of theorem 3.1.

■

4 Space discretization and applications

4.1 General setting

In order to compute the solution u^ε to (3.26), we find the profile $\mathcal{U}^\varepsilon$ given by the singular equation (3.31). We proceed as follows: let us give an initial data u_0^ε under the form $u_0^\varepsilon(x) = a(x)e^{i\frac{kx}{\varepsilon}} + c.c.$ with k given. We then choose ω such that the dispersion relation $\det(-i\omega + iAk + L_0) = 0$ is satisfied. Now, in order to approximate the solution (3.26), we use the semi-discretization (3.44) with initial data $\mathcal{U}^0(\theta, x) = e^{i\theta}a(x) + c.c.$ We still have to deal with the space discretization

of (3.44). One of the key point of the analysis of section 3 is that the linear part generates a unitary group. In order to ensure the same property at the discrete level, we use centered difference in space. Finally, the scheme reads:

$$\frac{\mathcal{U}_j^{n+1}-\mathcal{U}_j^n}{\delta t}+\left(A(D_0)+\frac{1}{\varepsilon}\mathcal{L}(\partial_\theta)\right)\frac{\mathcal{U}_j^{n+1}+\mathcal{U}_j^n}{2}=\Pi_{P_1}f(\mathcal{U}_j^n,\mathcal{U}_j^n),$$

where

$$\mathcal{U}_j^n=\sum_{k=-P_1}^{P_1}\mathcal{U}_{j,k}^n e^{ik\theta}$$

where $\mathcal{U}_{j,k}^n$ are real number and the operator $\mathcal{L}(\partial_\theta)$ is given by

$$\mathcal{L}(\partial_\theta)\mathcal{U}_j^n=\sum_{k=-P_1}^{P_1}\mathcal{L}(ik)\mathcal{U}_{j,k}^n e^{ik\theta},$$

and $A(D_0)$ denotes the centered difference operator

$$\left(A(D_0)\mathcal{U}^n\right)_j=\frac{A\mathcal{U}_{j+1}^n-A\mathcal{U}_{j-1}^n}{2\delta x}.$$

This is an implicit scheme with an explicit discretization of the nonlinearity. Moreover, at each time step $2P_1+1$ linear systems have to be solved. But since the solution is real, one has $\mathcal{U}_{j,k}^n=\overline{\mathcal{U}_{j,-k}^n}$, therefore one needs only to solve P_1+1 systems. In a 1-D geometry, these systems are solved by a direct method. In the next section, we present the application of our method to the second harmonic generation problem. We would like to emphasize that we obtain a discretization of the singular equation (3.31) (and therefore of the original system) and not one of an asymptotic solution.
No rigorous estimate of the error for the full discretization has been obtained. However, according to the numerical results of the next section, we can suggest that at least we should have

$$\sup_n ||\mathcal{U}_h^n(\theta,x)-\mathcal{U}(\theta,n\delta t,x)||=O(\varepsilon^{M_1}+\delta t+\delta x)$$

4.2 Application to second harmonic generation.

We consider again the Maxwell-Lorentz system (2.15) formulated as follows (the tildes have been omitted):

$$\partial_t H+\mathcal{M}\partial_z E=0, \tag{4.54}$$

$$\chi_\infty^{(1)}\partial_t E-\mathcal{M}\partial_z H+\frac{\omega_a}{\varepsilon}U+\frac{\omega_b}{\varepsilon}V=0, \tag{4.55}$$

$$\partial_t F - \frac{\omega_a}{\varepsilon} U = 0, \tag{4.56}$$

$$\partial_t G - \frac{\omega_b}{\varepsilon} V = 0, \tag{4.57}$$

$$\partial_t U + \frac{\omega_a}{\varepsilon} F - \alpha_a \frac{\omega_a}{\varepsilon} \mathcal{T} E = \omega_a \gamma J_a \chi^2(E, E), \tag{4.58}$$

$$\partial_t V + \frac{\omega_b}{\varepsilon} G - \alpha_b \frac{\omega_b}{\varepsilon} \mathcal{T} E = \omega_b \gamma J_b \chi^2(E, E). \tag{4.59}$$

We introduce $u^\varepsilon = (H, E, F, G, U, V)$ and the system satisfied by u^ε is of the form (3.26). On can therefore apply the methods of the previous section. However, the system (4.54)-(4.59) has a special structure: it can be reduced to a 6th order system as follows: one applies ∂_t on (4.58) and using (4.56) gives

$$\left(\partial_t^2 + \frac{\omega_a^2}{\varepsilon^2}\right) U - \alpha_a \frac{\omega_a}{\varepsilon} \mathcal{T} \partial_t E = \omega_a \gamma J_a \partial_t \chi^2(E, E). \tag{4.60}$$

The same operation on (4.59) using (4.57) leads to

$$\left(\partial_t^2 + \frac{\omega_b^2}{\varepsilon^2}\right) V - \alpha_b \frac{\omega_b}{\varepsilon} \mathcal{T} \partial_t E = \omega_b \gamma J_b \partial_t \chi^2(E, E). \tag{4.61}$$

We next compute ∂_t(4.55) and using (4.54) we obtain

$$\chi_\infty^{(1)} \partial_t^2 E + \mathcal{M} \partial_z^2 E + \frac{\omega_a}{\varepsilon} \partial_t U + \frac{\omega_b}{\varepsilon} \partial_t V = 0. \tag{4.62}$$

Now apply $\left(\partial_t^2 + \frac{\omega_a^2}{\varepsilon^2}\right)\left(\partial_t^2 + \frac{\omega_b^2}{\varepsilon^2}\right)$ on (4.62) and using (4.60)-(4.61) leads to

$$\begin{aligned} &\left(\partial_t^2 + \frac{\omega_a^2}{\varepsilon^2}\right)\left(\partial_t^2 + \frac{\omega_b^2}{\varepsilon^2}\right) \chi_\infty^{(1)} \left(\partial_t^2 + \mathcal{M}\partial_z^2\right) E, \\ &+ \left(\partial_t^2 + \frac{\omega_b^2}{\varepsilon^2}\right) \frac{\omega_a^2}{\varepsilon} \partial_t^2 \left(\frac{\alpha_a}{\varepsilon} \mathcal{T} E + \gamma J_a \chi^2(E, E)\right) \\ &+ \left(\partial_t^2 + \frac{\omega_a^2}{\varepsilon^2}\right) \frac{\omega_b^2}{\varepsilon} \partial_t^2 \left(\frac{\alpha_b}{\varepsilon} \mathcal{T} E + \gamma J_b \chi^2(E, E)\right) = 0. \end{aligned} \tag{4.63}$$

This system is a 6th order system equivalent to (4.54)-(4.59). Note that this elimination process can be performed for the singular equation, that is replacing ∂_t by $\partial_t - \frac{\omega}{\varepsilon}\partial_\theta$ and ∂_z by $\partial_z - \frac{k}{\varepsilon}\partial_\theta$. It can also be performed at the discrete level replacing ∂_t by differences in time and ω_a, ω_b, ∂_θ by mean values that is $\omega_a E$ is replaced by

$\omega_a \dfrac{E^{n+1}+E^n}{2}$ and $\partial_\theta E$ is replaced by $\partial_\theta \dfrac{E^{n+1}+E^n}{2}$. By this procedure, we have divided by a factor 6 the size of the matrices that have to be inversed at each time step. We obtain naturally a numerical scheme coupling directly 6 time-steps and that is equivalent to that of the previous section. Note that ω_a, ω_b, α_a, α_b are diagonal matrices that do not commute with $\mathcal{M}$.

For the numerical tests, we study a boundary value problem. The electric field for all times at $z = 0$ is given by

$$E(t, z = 0) = e^{i\frac{\omega t}{\varepsilon}} b(t) + c.c.$$

4.3 Numerical results.

4.3.1 Moving computational window

In order to reduce the computer resources required for the simulations, the pulse is tracked and computations are performed only where it is needed. For the clarity of the presentation, let us suppose that we have a global grid for the total computational domain and the grid points are numbered from 0 to $N_s + 1$ (from left to right). This is an artificial grid that will not be used in the practice because it can require a large memory space. However it allow a simple presentation of the adaptive window approach. In this global grid, the computational window, at each step n, is defined by the indexes I_l^n and I_u^n. These bounds are computed in order to satisfy the inequalities $1 \leq I_l^n < I_u^n \leq N_s$, and such that the electric field vanishes for all indexes out of the computational window:

$$\mathcal{E}_i^n = 0 \quad \text{for} \quad I_l^n \leq i \leq I_u^n$$

The tracking procedure is achieved by an estimation of the fastest v_f and the slowest v_s group velocities associated to the pulse. These velocities are estimated according to the light velocity, the angular velocities ω_a and ω_b and the permeability tensors ($\chi_s^{(1)}$ and $\chi_\infty^{(1)}$). It is possible to define the evolution of $I_l(n)$ and $I_u(n)$ so as to satisfy the relations:

$$0 \leq I_l^{n+1} - I_l^n \leq 1, \quad 0 \leq I_u^{n+1} - I_u^n \leq 1, \quad \text{and} \quad I_u^n - I_l^n = N_c.$$

where N_c is the size of the mesh in the moving computational window. For a short pulse propagating on a relative long distance, the size N_c is small compared to the equivalent fixed computational domain size N_s. Then, the moving window strategy improves considerably the computational time required.

4.3.2 Boundary conditions

For numerical applications the crystal will be supposed defined for $x = 0$ to $x = L_c + N_c\delta x$, where L_c is the crystal length and $N_c\delta x$ the size of the window of

computation. We assume that there is no electric field in the crystal at the initial time and the propagation is initiated by a the electric field $\mathcal{E}_0(t)$ defined at the point $x = 0$:

$$\mathcal{E}_0(t) = \frac{||\mathcal{E}_0||}{2}\mathcal{E}e^{-\frac{1}{2}\frac{t-4T_*}{T_*}^2}e^{-i\omega(t-4T_*)} + cc., \quad \forall t \geq 0,$$

where c is the light speed, T_* is time duration of the pulse, $||\mathcal{E}_0||$ is the strength of the pulse, $\mathcal{E}$ the polarization unit vector. In the non dimensional form, we have:

$$\mathcal{E}_0(t) = \frac{1}{2}\mathcal{E}e^{-\frac{1}{2}\frac{t-4T_*}{T_*}^2}e^{i\frac{\omega T_*}{\varepsilon}}e^{i\theta} + cc. \quad \text{for} \quad \theta = \theta(t, x = 0).$$

Therefore

$$\mathcal{E}_{0,p}(t) = \begin{cases} \frac{1}{2}\mathcal{E}e^{-\frac{1}{2}\frac{t-4T_*}{T_*}^2}e^{i\frac{\omega T_*}{\varepsilon}} & \text{if} \quad p = 1 \\ 0 & \text{if} \quad p \neq 1 \end{cases}$$

We also need to define the magnetic field $\mathcal{H}_0(t)$ at the left of the crystal. We will consider the following linear approximation:

$$\mathcal{H}_0(t) = \frac{k}{\omega}\mathcal{M}\mathcal{E}_{0,p}(t).$$

When new points comes in the computational window, according to the initial condition, associated unknowns are set to zero.

4.4 Applications.

In order to validate the numerical strategy proposed in this paper, some characteristic regimes of the conversion process are investigated. Computations are performed for a boundary value problems with a given incident wave at the left of the crystal and no field at the right. We assume that the incident pulse have a Gaussian shape. Its duration is $T_* = 150fs$, the wavelength is $\lambda = \frac{2\pi c}{\omega} = 815\,nm$ and the amplitude of the incident field is given by $||\mathcal{E}_0|| = 7.5\ 10^8 V/m$. According to the experimental results proposed in [21], the third order nonlinear effects are overlooked, and the coefficients of the quadratic polarization is:

$$\chi^{(2)} = d_{31} = d_{24} = d_{36} = 4(4.35\ 10^{-13})m/V.$$

Computations are performed with different mesh size, from $\delta x \simeq 6\lambda$ to $\delta x \simeq 0.5\lambda$. In all the figures below, all the fields are normalized by the amplitude $||\mathcal{E}_0||$ of the incident field.

The first regime considered for the numerical computations is the case of an incident wave satisfying the phase matching conditions. As the pulse propagate in the KDP crystal, the second harmonic ($p = 2$) is generated and amplified (Figure 1). After $700\mu m$ propagation, the fundamental ($p = 1$) and the second harmonic

waves sizes are of the same order. The pulse is dominated by the second harmonic component ($p = 2$) after $2000\mu m = 2mm$ propagation in the KDP crystal (Figure 2). In order to investigate the accuracy of the numerical approach, computations are performed for different mesh sizes (Figure 3). When the second harmonic generation is observed in terms of the energy conversion, there are no significant difference between coarse and fine meshes during the propagation in a 2000μ crystal. We can suppose that these results are associated to some conservative properties of the physical model, preserved by the numerical scheme. However, the details of the pulse evolution shows some important differences in the computations. Indeed, the converged pulse shape, until $\simeq 2000\mu m$ propagation in the KDP crystal, is obtained with fine meshes ($\delta x \simeq 1.2\lambda$ and $\delta x \simeq 0.5\lambda$). For $\delta x \simeq 6\lambda$ (respectively $\delta x \simeq 3\lambda$) the evolution of the pulse shape is can be assumed converged until $\simeq 500\mu m$ (respectively $\simeq 1000\mu m$) propagation in the crystal (figure 4). We then deduce that, for a fixed mesh size, the accuracy of the pulse shape is inversely proportional to the distance of propagation. According to the analysis associated to this regime, the non oscillating component ($p = 1$) and the components associated to $p > 2$ (not plotted) are of size very small compare to the incident wave. Indeed, in this case only the fundamental and the second harmonic components are in the characteristic variety of the propagation operator. In this case, different computations performed with the phase bases associated to $M \geq 2$, approximatively gives the same results.

When the incident wave properties are far from the phase matching conditions, the situation is different. The size of the second harmonic is now of order $\varepsilon \simeq 10^{-4}$ and does not grow during the propagation (figure 6). The modification of the fundamental wave shape observed on figure 6 is associated to the linear dispersion. Accurate computations are also obtained with $M = 1$.

The last regime considered is designed to show that, even when a mode is not perfectly in the characteristic variety, the proposed approach gives an accurate description of his evolution. Indeed, let us consider an incident wave near the phase matching conditions. In this case the second harmonic mode is nearly resonant. During the propagation in the KDP crystal this mode is successively amplified and damped with a maximum amplitude lower than the fundamental component but larger than $\varepsilon \sim 10^{-4}$ (figures 7 and 8). Of course in this case, computations with $M = 1$ will not gives accurate results, even for very fine meshes. The angle for phase matching is $\varphi = 44,35$ degree. The computation presented here is with $\varphi = 44,05$. This small different has some large effects.

Acknowledgments : This work was partially supported by the European network HYKE, funded by the EC as contract HPRN-CT-2002-00282 and GDR EAPQ 2103 CNRS.

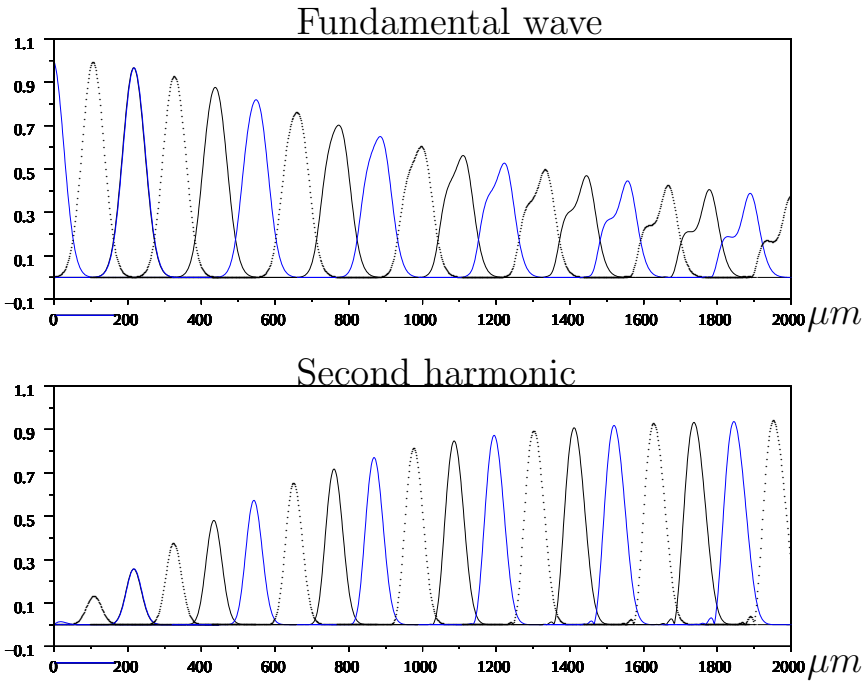

Figure 1: Case of an incident wave satisfying the phase matching conditions. Evolution of the normalized electric field shape as a function of the crystal thickness: Fundamental and second harmonic components.

References

[1] S. A. Akhmanov, V. A. Vysloukh, and A. S. Chrirkin, *Optics of Femtosecond Laser Pulses*. American Institute of Physics, 1992.

[2] H. J. Bakker, P.C.M. Planken, and H.G. Muller, Numerical calculation of optical frequency-conversion processes: a new approach. *JOSA B*, 6, 1989.

[3] B. Bidégaray, A. Bourgeade, D. Reigner, and R. W. Ziolkowski, Multilevel Maxwell-Bloch simulations. In *Proceeding of the Fifth Int. Conf. on Mathematical and Numerical Aspects of Wave Propagation*, pages 221–225, 2000. July 10-14, Santiago de Compostela, Spain.

[4] A. Bourgeade, Etude des propriétés de la phase d'un signal optique calculé avec un schéma aux différences finies de Yee pour un matériau linéaire ou quadratique. Preprint R-5913, CEA, Avril 2000.

[5] A. Bourgeade and E. Freysz. Computational modeling of the second harmonic generation by solving full-wave vector Maxwell equations. *JOSA*, 17, 2000.

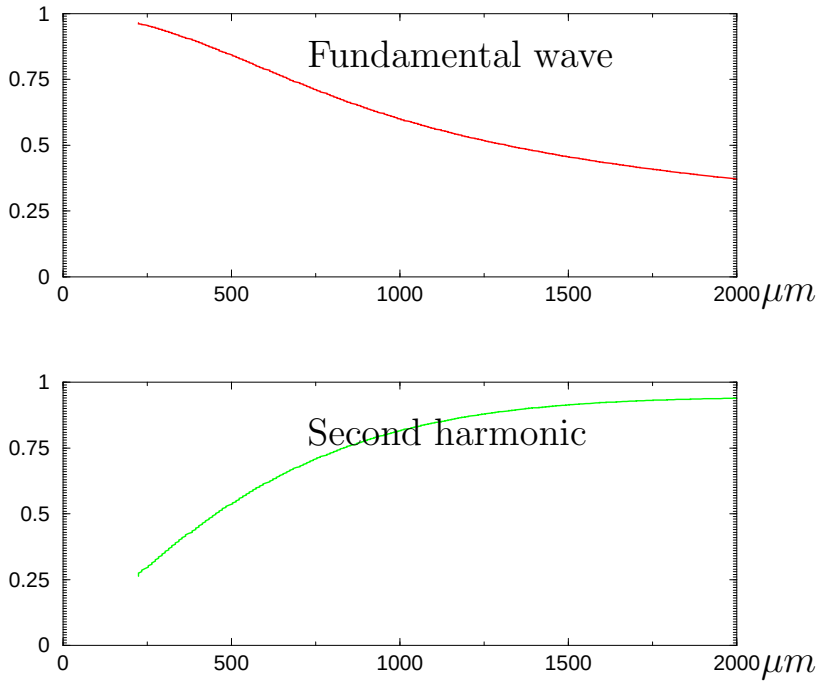

Figure 2: Case of an incident wave satisfying the phase matching conditions. Evolution of the normalized electric field amplitude as a function of the crystal thickness: Fundamental and second harmonic components.

[6] R. W. Boyd, *Nonlinear Optics*. Academic Press, 1992.

[7] T. Colin et P. Fabrie, *Semidiscretization in time for Schrödinger-waves equations*, Discrete and continuous dynamical systems, vol4, No 4, 671-690, (1998).

[8] T. Colin, C. Galusinski, H.G. Kaper, *Long waves in micro magnetism*, Communications in PDE, 27 (2002), no. 7-8, 1625–1658, 3.

[9] T. Colin and B. Nkonga, Numerical model for light interaction with two level atoms medium, Physica D, vol. 188, No 1-2, p.92-118, 2004.

[10] T. Colin and B. Nkonga, Computing oscillatory waves of nonlinear hyperbolic sytsems using a phase-amplitude approach. In *Proceeding of the Fifth Int. Conf. on Mathematical and Numerical Aspects of Wave Propagation*, page 954, 2000. July 10-14, Santiago de Compostela, Spain.

[11] P. Donnat, J.-L. Joly, G. Métivier and J. Rauch, *Diffractive nonlinear geometric optics,* Séminaire sur les équations aux Dérivées Partielles, 1995–1996, Exp. No. XVII. Ecole Polytech., Palaiseau, 1996.

[12] B. Fidel, E. Heymann, R. Kastner, and R.W. Ziolkovski, Hybrid ray-FDTD moving window approach to pulse propagation. *J. Comput. Phys.*, 138:480–500, 1997.

[13] L. Gilles, S. C. Hagness, and L. Vazquez, Comparison between staggered and unstaggered finite-difference time-domain grids for few-cycle temporal optical soliton propagation. *J. Comput. Phys.*, 16n1:379–400, 2000.

[14] C.V. Hile and W. L. Kath, Numerical solutions of Maxwell's equations for nonlinear-optical pulse propagation. *J. Opt. Soc. Am. B*, 13:1135–1145, 1996.

[15] J.-L. Joly, G. Métivier and J. Rauch, *Generic rigorous asymptotic expansions for weakly nonlinear geometric optics*, Duke Math. J. 70, 373-404, 1993.

[16] J.-L. Joly, G. Métivier and J. Rauch, *Transparent nonlinear geometric optics and Maxwell-Bloch equations*, Journal of Differential Equations 166, 175-250, 2000.

[17] R. M. Joseph and A. Taflove, FDTD Maxwell's equations models for nonlinear electrodynamics and optics. *IEEE Trans. Atennas and Propagation*, 45, 1997.

[18] N.C. Kothari and X. Carlotti, Transient second-harmonic generation: Influence of the effective group-velocity dispersion. *JOSA B*, 5, 1988.

[19] D. Lannes, *Dispersive effects for nonlinear geometrical optics with rectification*, Asymptotic Analysis 18, p.p. 111-146, 1998.

[20] A. C. Newell and J. V. Moloney, *Nonlinear Optics*. Addison-Wesley Publiching Compagny, 1991.

[21] R. Maleck Rassoul, A. Ivanov, E. Freysz, A. Ducasse, and F. Hache, Second harmonic generation under phase and group velocity mismatch. influence of cascading, self and cross phase modulations. *Opt. Letters*, 22, 1997.

[22] F. Rob Remis, On the stability of the finite-difference time-domain method. *J. Comput. Phys.*, 163(1):249–261, 2000.

[23] D.A. Russel, D.F. Dubois and H.A. Rose, Nonlinear saturation of stimulated Raman scattering in laser hot spots. *Physics of Plasmas*, 6 (4), 1294-1317, 1999.

[24] A. Taflove, *Computational Electrodynamics: The Finite-Difference Time-Domain Method*. Artech House, Norwood, MA, 1995.

[25] K. S. Yee, Numerical solution of initial boundary value problems involving Maxwell's equations in isotropic media. *IEEE Trans. Antennas and Propagation*, 14:302–307, 1966.

[26] D. W. Zingg, H. Lomax, and H. M. Jurgens, High-accuracy finite-difference schemes for linear wave propagation. *SIAM J. Sci. Comput.*, 17(2):328–346, 1996.

[27] W. D. Zingg, Comparison of high-accuracy finite-difference methods for linear wave propagation. *SIAM J. Sci. Comput.*, 22(2):476–502, 2000.

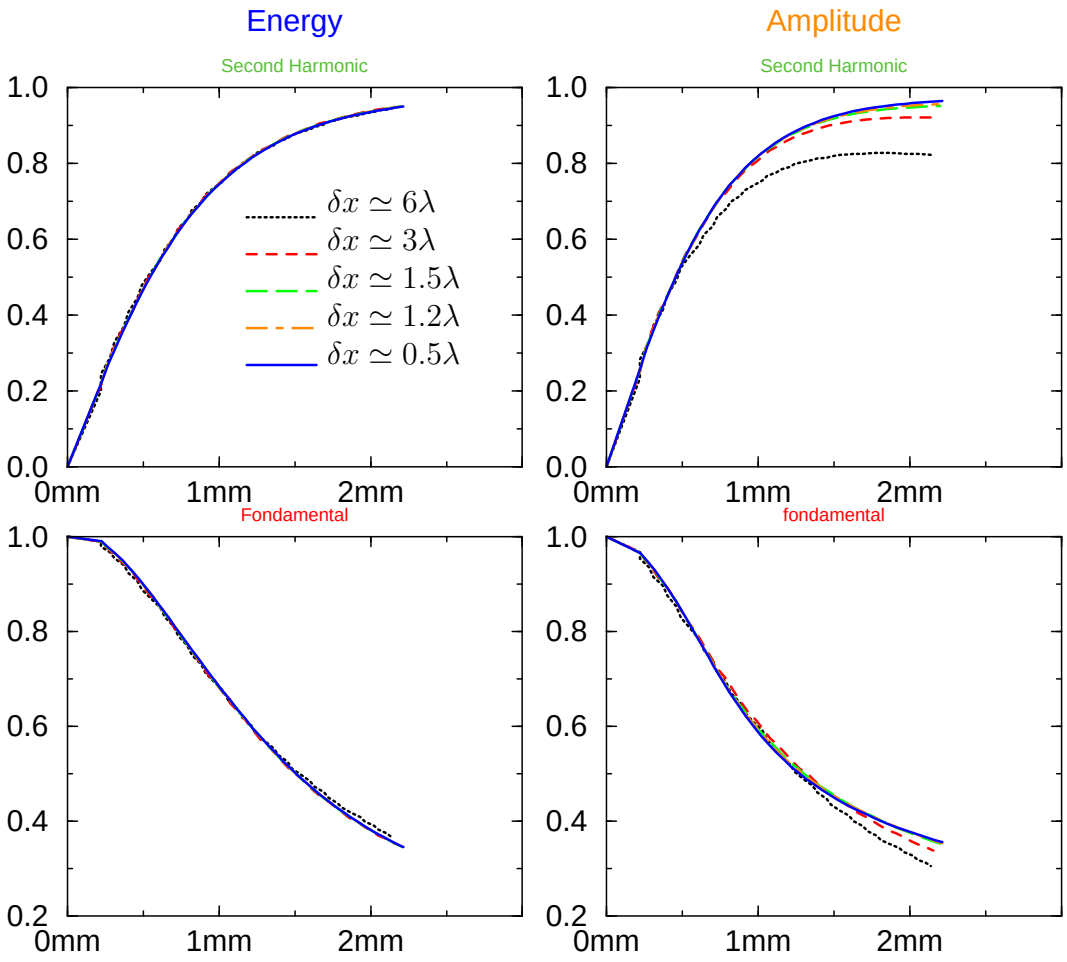

Figure 3: Case of an incident wave satisfying the phase matching conditions. Normalized energy (left) and amplitude (right) as a function of the crystal thickness: Fundamental and second harmonic components.

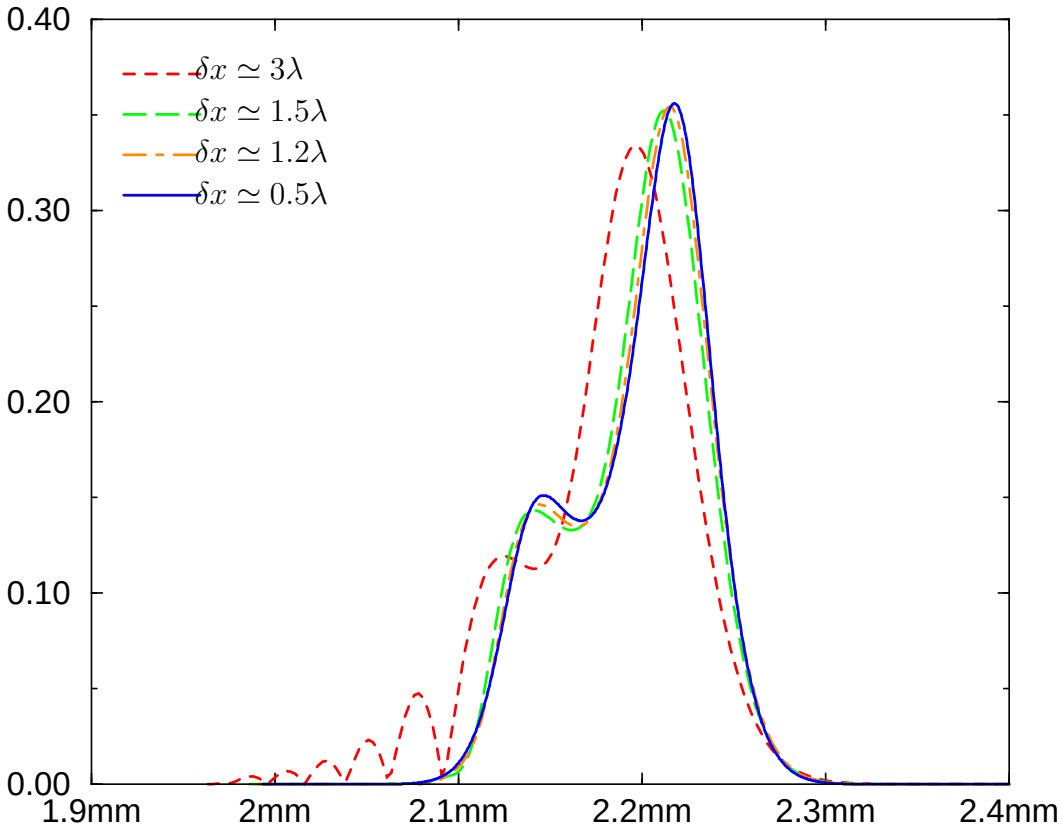

Figure 4: Case of an incident wave satisfying the phase matching conditions. Shape of the fundamental component of the electric field after $2mm$ propagation in a KDP crystal: mesh convergence investigation.

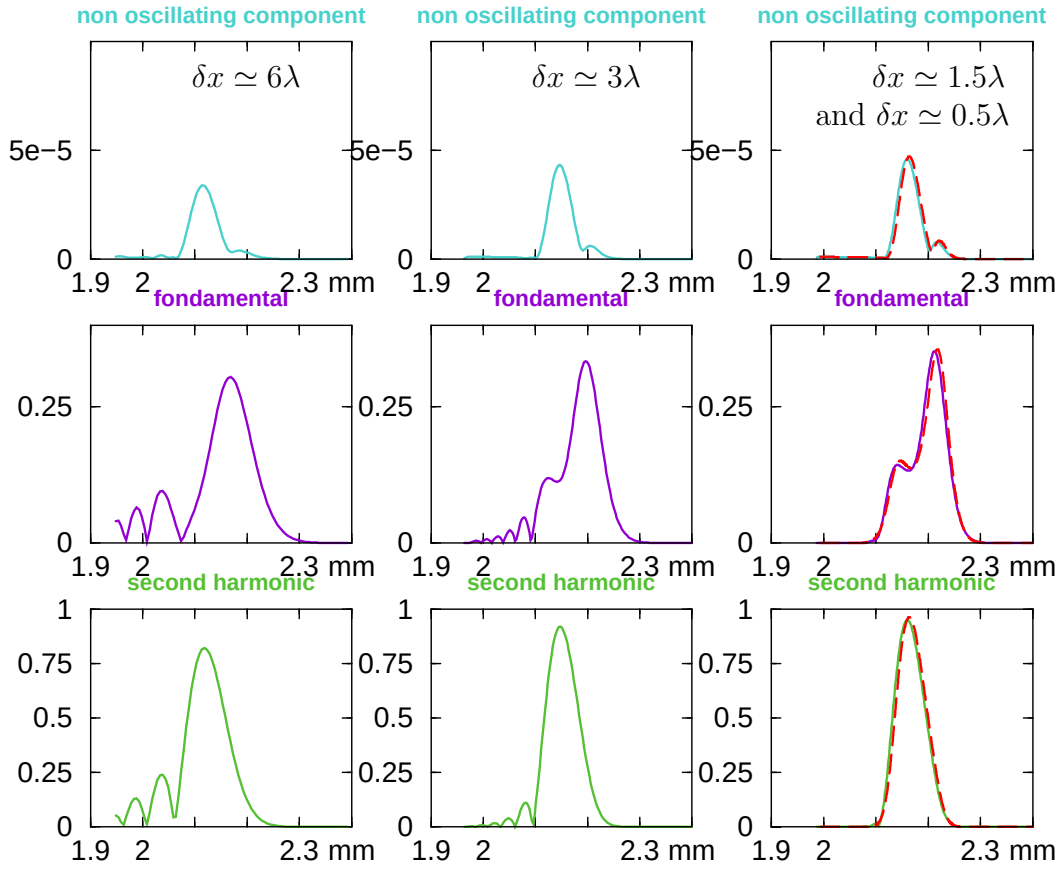

Figure 5: Case of an incident wave satisfying the phase matching conditions. Shape of the non oscillating (p=0), the fundamental (p=1) and the second harmonic (p=2) components of the electric field after $2mm$ propagation in a KDP crystal: mesh convergence investigation. From left to right $\delta x \simeq 6\lambda$, $\delta x \simeq 3\lambda$ and $\delta x \simeq 1.5\lambda$.

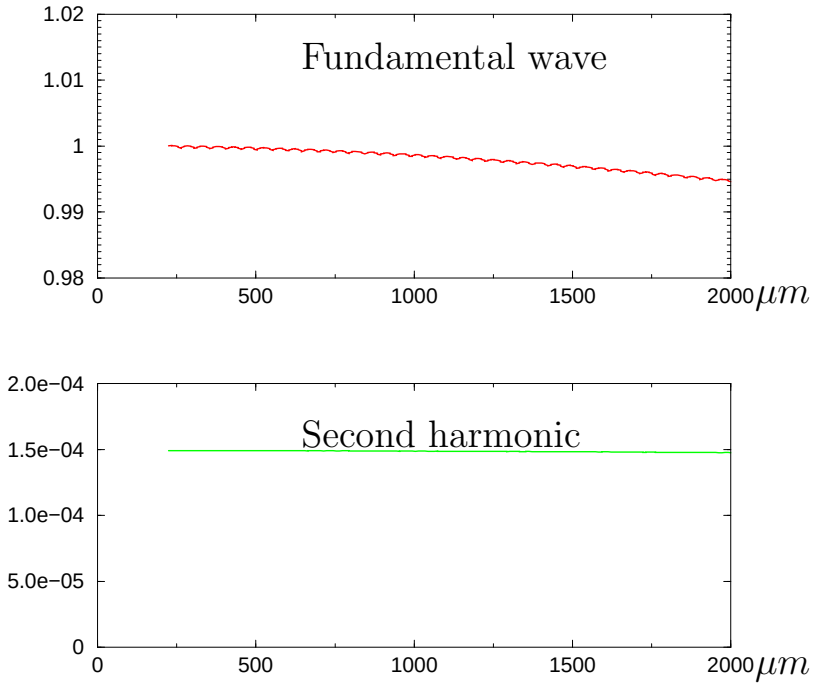

Figure 6: Case of an incident wave far from the phase matching conditions: Evolution of the normalized electric field amplitude in the crystal. Fundamental (p=1) and the second harmonic (p=2) components.

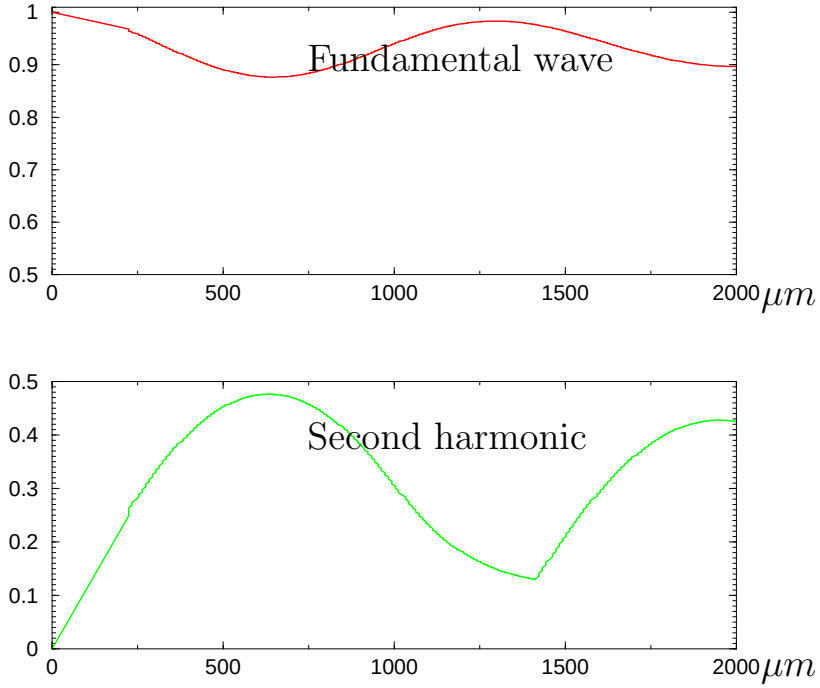

Figure 7: Case of an incident wave near the phase matching conditions: Evolution of the normalized electric field amplitude in the crystal. Fundamental (p=1) and the second harmonic (p=2) components.

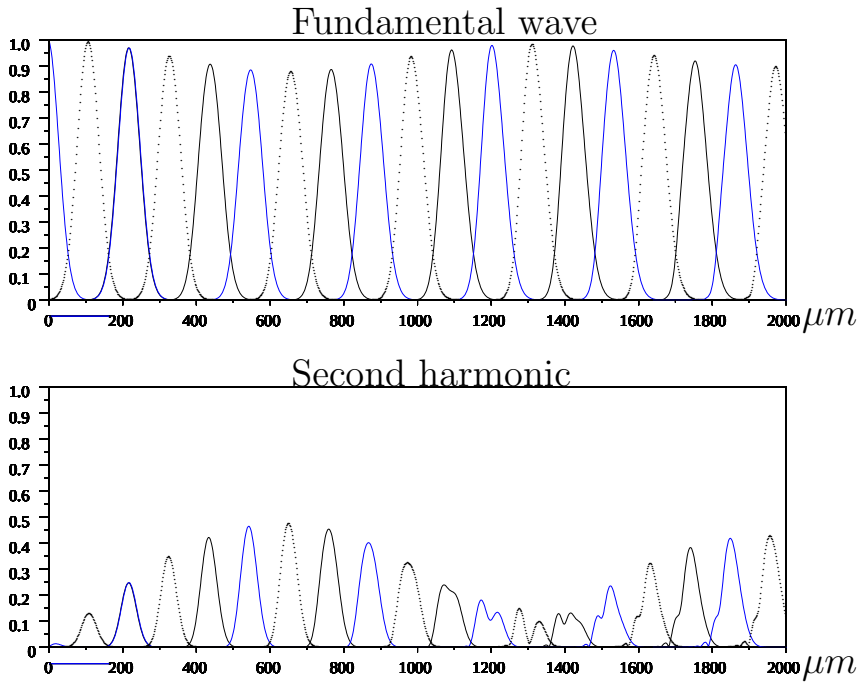

Figure 8: Case of an incident wave near the phase matching conditions: Evolution of the normalized electric field amplitude in the crystal, fundamental (p=1) and the second harmonic (p=2) components.